KD 6290-EE-01

(2)

AD

MOLECULAR FILMS FOR OPTOELECTRONICS

Final Technical Report

by

Professor J.O. Williams
(Principal Investigator)

Professors L E Davis, R W Munn, J H R Clarke and T A King
(Co-Investigators)

September 1992

United States Army

EUROPEAN RESEARCH OFFICE OF THE U.S. ARMY

London England

CONTRACT NUMBER DAJA 45-89-C-0036

Contractor : UMIST, Manchester, U.K.

Approved for Public Release; distribution unlimited

lassified
/ CLASSIFICATION OF THIS PAGE

REPORT DOCUMENTATION PAGE

ORT SECURITY CLASSIFICATION lassified	1b. RESTRICTIVE MARKINGS
URITY CLASSIFICATION AUTHORITY	3. DISTRIBUTION / AVAILABILITY OF REPORT Approved for public release; distribution unlimited
LASSIFICATION / DOWNGRADING SCHEDULE	
ORMING ORGANIZATION REPORT NUMBER(S)	5. MONITORING ORGANIZATION REPORT NUMBER(S) R&D 6290-EE-01
ME OF PERFORMING ORGANIZATION iversity of Manchester stitute of Science & Tech. — 6b. OFFICE SYMBOL (If applicable)	7a. NAME OF MONITORING ORGANIZATION European Research Office USARDSG-UK
RESS (City, State, and ZIP Code)). Box No. 88 ichester, M60 1QD	7b. ADDRESS (City, State, and ZIP Code) PSC 802 Box 15 FPO AE 09499-1500
ME OF FUNDING / SPONSORING ANIZATION ropean Research Office ARDSG-UK ARO-E — 8b. OFFICE SYMBOL (If applicable)	9. PROCUREMENT INSTRUMENT IDENTIFICATION NUMBER DAJA45-89-C-0036
DRESS (City, State, and ZIP Code) C 802 Box 15 O AE 09499-1500	10. SOURCE OF FUNDING NUMBERS PROGRAM ELEMENT NO. 0601102A — PROJECT NO. 1L161102BH57 — TASK NO. 03 — WORK UNIT ACCESSION NO.
LE (Include Security Classification)) Molecular Films for Opto-Electronics	
SONAL AUTHOR(S) ofessor J.O. Williams	
PE OF REPORT nal — 13b. TIME COVERED FROM 1.10.89 TO 30.6.92 — 14. DATE OF REPORT (Year, Month, Day) 24 September 1992 — 15. PAGE COUNT 40	
PLEMENTARY NOTATION	

COSATI CODES			18. SUBJECT TERMS (Continue on reverse if necessary and identify by block number)
LD	GROUP	SUB-GROUP	Langmuir-Blodgett film, nonlineara optics, optoelectronics, molecular dynamics, second-harmonic generation, SHG,
05			
06			

STRACT (Continue on reverse if necessary and identify by block number)

lecular dynamics computer simulations have been used to model monolayer and trilayer ngmuir-Blodgett films formed by model amphiphilic molecules. Several factors have been entified that control film structure and stability, thus giving insight into optimum lecular design. Head-groups and the substituent position of hydrocarbon chains should be signed to maximise the stability of layer-like packing. Molecular tilt is an important ctor since it results in local structural defects and roughening of interfaces which uld lead to formation of long range inhomogeneities.

nerical calculations of non-linear optical response have been performed fro model LB lms in which molecules are treated as rigid strings of beads to represent their size, ape and orientation. Interactions between molecules are obtained as planewise dipole ns which prove to be negligible except within a layer. Although the local fields vary

STRIBUTION / AVAILABILITY OF ABSTRACT UNCLASSIFIED/UNLIMITED ☒ SAME AS RPT. ☐ DTIC USERS	21. ABSTRACT SECURITY CLASSIFICATION Unclassified
AME OF RESPONSIBLE INDIVIDUAL . K. Steinbach	22b. TELEPHONE (Include Area Code) 071 409 4423 — 22c. OFFICE SYMBOL AMXSN-UK-RI

ORM 1473, 84 MAR — 83 APR edition may be used until exhausted. All other editions are obsolete.

Block 18, continued.

amphiphile, planewise dipole sum.

Block 19, continued.

little with tilt so that the optical properties of the film depend primarily on the molecular response referred to the film axes, the pattern of nonlinear response is sensitive to molecular tilt.

In parallel with the theoretical work experimental studies have been performed on selected candidates fro practical LB films with good optoelectronic properties. Detailed studies sho the stearyl derivatives of DAN, MAP and NPP retain strong SHG activity but difficulties were encountered in forming satisfactory films.

DAJA-89-C-0036
ATTACHMENT 2

REPORT DOCUMENTATION PAGE

ERO Proposal Number: Contract Number: DAJA-45-89-C-0036

Title of Proposal: **MOLECULAR FILMS FOR OPTO-ELECTRONICS**

Report Number: Final Period Covered: From 1.10.89 To 30.6.92

Name of Institution: UMIST
PO BOX 88
MANCHESTER, M60 1QD

Principal Investigator: PROFESSOR J O WILLIAMS

Abstract: (Approximately 75 words for Interim Report; 300 for Final)

Molecular dynamics computer simulations have been used to model monolayer and trilayer Langmuir-Blodgett films formed by model amphiphilic molecules. Several factors have been identified that control film structure and stability, thus giving insight into optimum molecular design. Head-groups and the substituent position of hydrocarbon chains should be designed to maximise the stability of layer-like packing. Molecular tilt is an important factor since it results in local structural defects and roughening of interfaces which could lead to formation of long range inhomogeneities.

Numerical calculations of non-linear optical response have been performed for model LB films in which molecules are treated as rigid strings of beads to represent their size, shape and orientation. Interactions between molecules are obtained as planewise dipole sums which prove to be negligible except within a layer. Although the local fields vary little with tilt so that the optical properties of the film depend primarily on the molecular response referred to the film axes, the pattern of nonlinear response is sensitive to molecular tilt.

In parallel with the theoretical work experimental studies have been performed on selected candidates for practical LB films with good optoelectronic properties. Detailed studies show the stearyl derivatives of DAN, MAP and NPP retain strong SHG activity but difficulties were encountered in forming satisfactory films.

USARDSG Form 1188

List of contents

MOLECULAR FILMS FOR OPTOELECTRONICS

Statement of the problem investigated

This experimental and theoretical research program was aimed at the optimisation of Langmuir-Blodgett films for optoelectronic applications. The work falls into three areas:

1. Molecular dynamics computer modelling

The aim here was to understand how the structure of multilayer LB films is controlled by the intermolecular forces between the constituent amphiphilic molecules, and in this way to provide guidelines for the design of stable films for optoelectronic applications. On the basis of the results obtained from the simulation studies we have been able to identify several factors which control the stability and structure of LB films.

2. Theoretical calculations

The aim was to determine how the nonlinear optical response of molecules that form LB films expresses itself in the nonlinear optical response of the films. An understanding of this problem can help guide molecular design for optimal nonlinear optical response. The problem was addressed by performing theoretical calculations on simplified model structures. A key feature of the method was the use of planewise dipole lattice sums to treat the interactions between layers.

3. Synthesis, deposition and characterisation of LB films formed by p-nitroaniline derivatives.

Single crystal para-nitroaniline molecules are known to form crystals with high non-linear optical response. Selected examples were:

DAN - 4-N,N-dimethylamino-3-acetimidonitrobenzene
MAP - 2,4-dinitrophenyl-1-alanine methyl ester
NPP - (s)-N-(4-nitro-phenyl)-prolinol.

The aim was to synthesise stearyl derivatives to produce amphiphilic molecules SDAN, SMAP and SNPP which can be formed into Langmuir-Blodgett films. Linear and non-linear optical properties of stable films were then characterised.

Summary of major results

(Details of the methods and techniques used and results obtained are given later in this report)

(a) Programs for molecular dynamics simulation of multilayer LB films and for the calculation of planewise dipole sums for layered structures have been written and tested against previous data.

(b) Simplified but computationally tractable models have been used which reflect the essential molecular features of the amphiphilic molecules. The head groups and the methylene groups of the tails have been represented by single interaction sites with appropriately chosen parameters. This "first approximation" model has helped us to understand how various molecular factors control structure.

(c) This molecular model has been used to simulate and characterize monolayers on a flat surface and this work is now published [M. Bishop and J. H. R. Clarke, J. Chem. Phys., 95, 540 (1991)].

(d) We have studied Y-type trilayer LB films at 200K and 300K and preliminary reports of this work have been published. The films were built and equilibrated layer by layer with the heads of the first layer pointing towards the surface. Each trilayer "unit cell" contained 192 chains with periodic boundary conditions were imposed in the directions parallel to the surface.

(e) The tails stay predominantly in the all trans configuration at the close packed densities of LB films. As the size of head groups increases the available spare volume for the chains is filled by tilting. The mean tilt angles are in agreement with the prediction of the simple constant projected area model. The similarity between collective and mean tilts is evidence for strong correlation between molecular orientations within a layer although there is little correlation in the direction of tilt between adjacent layers. This may be related to the lack of orientation dependent forces between the head groups.

(f) The fraction of gauche defects is small but nevertheless increases with increasing tilt. For the hydrophobic interface between chain ends this can lead to chain interpenetration and interface roughness. This promotes the formation of defective regions in the long range lateral structure.

(g) The density profile across the film reveals significant disorder in the head group interface between the second and third layers which is in broad agreement with recent experimental measurements using atomic force microscopy [J. Garnaes, D.K. Schwatz, R. Viswanathan and J.A.N. Zasadrinski, Nature, 357, 54 (1992)]. This can be related to the general metastability of these layer structures which, for spherical head groups, results in spontaneous buckling of the interface.

(h) Model film structures have been devised that incoporate close packing of the molecules, represent the elongated shape of the molecules and allow for tilt of the molecules away from the normal to the film.

(i) Calculations of planewise dipole sums have been performed for various structure. Once the molecules become sufficiently elongated (axial ratio >5), further elongation makes little difference. In particular the interactions between molecules in different layers prove to be negligible even in markedly tilted structure, which simplifies the algebraic theory.

(j) Algebraic expressions have been derived for the local polarizing field, the macroscopis electric field, the linear susceptibility, the relative permittivity, the refractive indices, and the quadratic and cubic nonlinear susceptibilities. Because of the weak interactions between planes, the results for sequences of different layers are simple combinations of those for individual layers.

(k) Simplified values of the molecular polarisability and hyperpolarisability components have been used in numerical calculations of the film properties in (k). The local fields show surprisingly little dependence on molecular tilt, so that the susceptibilities reflect mainly the effect of tilt on these molecular responses. Distortions in the layers have little effect.

(l) Tilt complicates the *pattern* of components of the nonlinear susceptibilities. In the cubic susceptibility, the "cascading" contribution due to the first hyperpolarizability β can be comparable in magnitude to the "direct" one due to the second hyperpolarizability γ, so that the former should not be ignored.

(m) Synthetic schemes and purification procedures were developed for preparing the stearyl derivatives. All three materials are crystalline solids at room temperature.

(n) The crystalline powders still exhibit SHG so that the addition of stearyl groups does not induce centrosymmetry.

(o) Floating monolayers were characterised by p-A isotherms and Langmuir-Blodgett films by X-ray diffraction, UV/visible spectroscopy and optical measurements

(p) SDAN was found to form X, Y and Z-type films on silanised glass plates dependent on the subphase conditions.

(q) Although SNPP exhibits well-defined p-A isotherms, the transfer of films on to solid substrates is difficult and produces less reliable results.

(r) For SMAP no conditions have been found that give a floating monolayer, even in mixtures with behenic acid which is strongly film-forming.

(s) For LB films of SDAN the SHG coefficient is about 10% of that of the DAN crystal. SNPP shows similar behaviour relative to NPP whilst preliminary measurements on SMAP show very high conversion efficiencies although there is evidence of microcrystallite formation.

Conclusions

To avoid disordering effects in multilayer films the optoelectronically-active head groups and the position of substituent alkyl chains should be carefully designed to maximise the natural stability for layer-like packing. The frequent absence of relevant experimental data emphasises the importance of atomistic molecular mechanics studies for exploring this criterion. Strong interactions can cause the head groups to leave the surface in an attempt to form more stable aggregates. The effect is frustrated by the chain interactions but can nevertheless give rise to considerable interfacial disorder. The large size of head groups can lead to an increase in chain disorder and consequent chain penetration effects which give rise to roughening of the tail-tail interface. These effects could be alleviated by designing multiple chain amphiphiles.

Theoretical calculations show that local electric fields vary little with tilt so that the optical properties of the film depend mainly on the molecular response referred to the film axes. The pattern of nonlinear reponse does however vary significantly with molecular tilt. The results form a basis for treatments of more realistic models in which the response is not uniformaly distributed but is concentrated in the NLO chromophore. In combination with the molecular dynamics modelling of structure, such studies offer a systematic approach to molecular design for highly active LB films.

The preparation and purification of the stearyl derivatives has been performed for several candidate molecules. Although much of the NLO activity is retained the production of stable multilayer films of high optical purity requires further work on the detailed design of these molecules utilising results of the modelling and theoretical calculations.

Personnel

Professor J.O. Williams had overall direction of the research.

Professor J.H.R. Clarke directed the research on the modelling of LB films and was involved in program development for the molecular dynamics calculations.

Dr. M. Bishop (Research Associate) was employed to write computer programs and perform the molecular dynamics simulations

Mr. A. Baggaley (Ph.D. research student) has performed some of the latest simulations on LB trilayers.

Professor R.W. Munn directed the work on on theoretical calculations and performed most of the algebraic manipulations.

Dr. M.M. Shabat (Research Associate) was employed to perform the bulk of the theoretical calculations.

Mr. S.J. Collins and Mr. J.C. Boxall (undergraduates) performed calculations on distorted structures as projects.

Dr. F.R. Mayers performed the experimental work on SDAN

Mr. O. Szczur performed the experimental work on SMAP and SNPP.

Professors L.E. Davis and T. King directed work on the measurement of nonlinear optical properties.

List of Publications

M. Bishop and J. H. R. Clarke, System size dependence and time convergence in molecular dynamics simulations of monolayer films, *J. Chem. Phys.*, 95, 540 (1991).

M. Bishop, J.H.R. Clarke, L.E. Davis, T.A. King, F.R. Mayers, A Mohebati, R.W. Munn, M.M. Shabat, D. West and J.O. Williams, Structure and non-linear properties of LB films from *p*-nitroaniline derivatives,
Thin Solid Films 210/211, 185 (1992).

M. Bishop, J.H.R. Clarke, L.E. Davis, T.A. King, F.R. Mayers, A Mohebati, R.W. Munn, M.M. Shabat, D. West and J.O. Williams, Design of Langmuir-Blodgett films for non-linear optics,
presented at the *European Conference on Molecular Electronics* (Padua 1992)
to be published in *Molecular Crystals and Liquid Crystals*

A. Baggaley, M. Bishop and J.H.R. Clarke, Molecular dynamics simulation of trilayer Langmuir-Blodgett films, to be submitted to *J. Chem. Phys.*

R.W. Munn, S.E. Mothersdale and M.M. Shabat, Theory of nonlinear optical response in molecular layers.
Organic Materials for Nonlinear Optics II, ed. R.A. Hann and D. Bloor, Royal Society of Chemistry Special Publication no. 91, (Royal Society of Chemistry , London 1991), pp. 34-40

R.W. Munn and M.M. Shabat, Calculations of nonlinear optical properties of model LB films, *Molecular Electronics - Science and Technology II*, ed. A. Aviram, AIP Conference Proceedings 262 (American Institute of Physics, New York, 1992), 245-251

R.W. Munn and M.M. Shabat, Calculations of nonlinear optical response in LB films, presentation at conference *Organic materials for Nonlinear Optics III* (Oxford, 1992), to be published as a Royal Society of Chemistry Special Publication.

[further articles describing our results are in preparation or planned]

Structure and nonlinear optical properties of Langmuir–Blodgett films from *p*-nitroaniline derivatives

M. Bishop[a], J. H. R. Clarke[a], L. E. Davis[b], T. A. King[c], F. R. Mayers[a], A. Mohebati[c], R. W. Munn[a], M. M. Shabat[a], D. West[c] and J. O. Williams[a]

Departments of [a]Chemistry and [b]Electrical Engineering and Electronics, UMIST, Manchester M60 1QD (U.K.)

[c]Department of Physics, University of Manchester M13 9PL (U.K.)

Abstract

Stearyl derivatives of DAN, MAP and NPP yield LB films with second-harmonic generation (SHG) coefficients measured as 7, 100 and 20×10^{-9} esu. Molecular dynamics modelling predicts molecular tilts of about 20°, decreasing slightly in successive layers. Model calculations show how molecular tilt affects film optical response.

1. Introduction

This paper presents results from a coordinated programme to design, prepare and characterize LB films with high nonlinear optical (NLO) activity. The single crystal *para*-nitroaniline derivatives DAN [1], MAP [2] and NPP [3] exhibit encouraging efficiencies for frequency doubling of laser radiation. We have therefore synthesized further derivatives yielding Langmuir–Blodgett (LB) films with potentially high SHG efficiencies, and have explored how molecular structural features affect film structure and nonlinear optical behaviour.

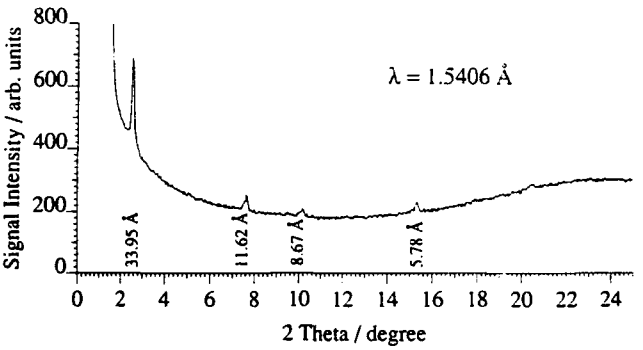

Fig. 1. X-ray diffraction spectrum from a Z-type LB film of SDAN.

2. Materials, film deposition and characterization

Suitable derivatives must retain the optical characteristics of the parent NLO molecule but yield ordered, homogeneous, noncentrosymmetric LB films. Incorporation of the stearyl moiety gave the compounds SDAN, SMAP, and SNPP, which achieved these aims. Even the powders gave frequency doubling, showing that judicious addition of a long hydrocarbon chain to the active centre need not render the material NLO inactive, as happens with some other derivatives [4]. The materials also demonstrated good LB film forming properties and short cut-off wavelengths in the visible.

X-ray diffraction spectra from multilayer LB films of these materials on silanized glass substrates show a large number of d_{00l} reflections for each material, indicating that they are highly ordered (Fig. 1). For most films the transfer ratio and large d_{00l} spacing exclude X or Z type film formation, but for SDAN under some conditions both X and Z type films appear to be possible. There seems to be a variation of molecular orientation for some films, ranging from near vertical to a tilt of about 30°, depending on the dipping temperature and pH.

3. Optical properties and measurement of SHG

The unpolarized UV/visible absorption spectra show that the cut-off is below 450 nm for each material. For SHG the incident light was the 1064 nm wavelength from a Q-switched Nd : YAG laser producing pulses of 2 mJ energy and 10 ns duration, focused down to about 200 μm spot size and p-polarized. The p-polarized harmonic signal was detected in transmission as a function of angle of incidence (Fig. 2) through low wavelength pass filters, a 532 nm bandpass filter of 1 nm bandwidth and neutral density filters of appropriate optical density, using a gated photomultiplier tube. A nonzero signal is observed at normal incidence indicating noncentrosymmetry in the plane of the film. Quartz

0040-6090/92/$5.00

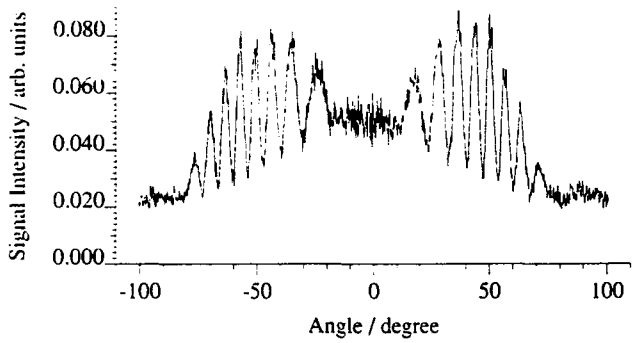

Fig. 2. Second-harmonic signal as a function of angle of incidence to the sample film.

Maker fringes were used as a calibration standard for measuring SHG d coefficients. The values obtained for $d/10^{-9}$ esu were 7 for SDAN, 100 for SMAP and 20 for SNPP.

4. Molecular dynamics simulations

Our simulations aim was to understand how interactions between molecules control the structure of multilayer LB films. We have extended previous monolayer studies [5–7] to investigate Y type trilayers with 192 chains, to assess how molecular orientation in the first layer influences the packing in subsequent layers.

Despite their apparent chemical complexity, the molecules of interest can be adequately represented by a large single interaction site (the NLO-active aromatic head group) combined with a set of 17 connected sites (the CH_2 groups on the hydrocarbon tail). Lennard–Jones 12–6 potentials were used [5, 7] to represent the site interactions. Values of the Lennard–Jones parameters ϵ_h/k_B, σ_h and the head-group mass (100 K, 4.238 nm and 0.050 kg mol^{-1}) were selected to correspond roughly [6] to stearic acid.

The chain was kept connected in the dynamics by constraining the hydrocarbon tail to 0.153 nm between sites and $(\sigma_h + \sigma_t)/2$ between the head and the first site. The bond angle, torsion angle and surface potentials were as in our previous study [7]. The first 16 000 time steps (40 ps) were discarded for equilibration; the subsequent production run lasted 40 ps.

The mean tilt angles in the three layers were $20.62 \pm 0.08°$, $19.40 \pm 0.10°$ and $18.42 \pm 0.08°$ at a surface coverage of 19.6 Å^2 per chain, very close to that obtained from our monolayer studies [7], $20.34° \pm 0.04°$. The density $G(z)$ normal to the $z = 0$ plane is shown in Fig. 3. The first layer is highly ordered, with a sharp first peak arising from the head-group locations. The corresponding peaks in the second and third layers become increasingly broader, suggesting increasing roughening of the head-group layers.

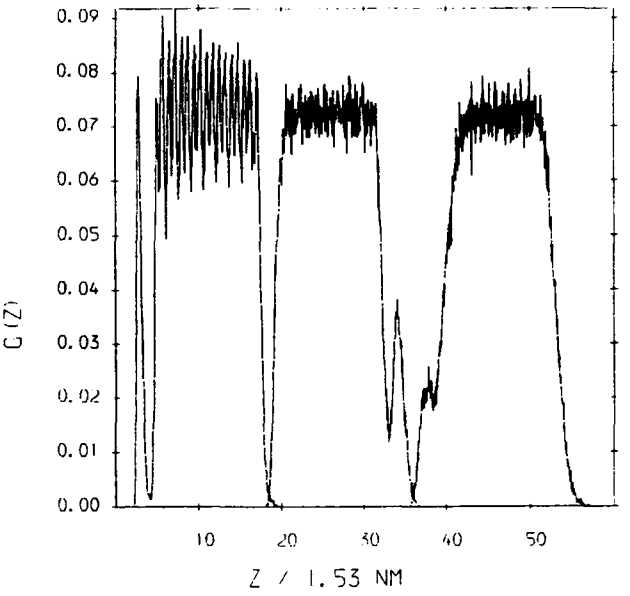

Fig. 3. The density profile normal to the $z = 0$ plane for the trilayer system. $G(z)$ is normalized so that the area under the curve for each layer is unity. Distances are quoted as multiples of the hydrocarbon C–C bond length.

5. Theory of film NLO response

The nonlinear optical response of ordered films can be calculated from the molecular hyperpolarizability β, the molecular orientation, and the local electric fields in the layers. In turn, the local fields depend on sums of dipole tensor interactions between a molecule in one layer and all the molecules in that or another layer [8]. Calculations of these planewise dipole sums L have been performed for a series of close-packed model structures. The molecules are represented as spherocylinders of diameter D and length sD and are treated as a set of s equally spaced centres between which the interactions are averaged. The molecules may be oriented normal to the layers or tilted at an angle θ to the vertical. Interactions between a molecule and those in its own plane dominate for all values of s studied, with interactions beyond the neighbouring layer negligible. For $s = 5$, the in-plane sums for molecules tilted towards the next-nearest neighbours (consistent with the results from the dynamic modelling) vary as shown in Table 1, where x is the next-nearest-neighbour direction. The tilt lowers the symmetry from hexagonal to monoclinic, but off-diagonal elements remain small.

For a single layer, the local-field tensor $\boldsymbol{d}$ is given by $(1 - \boldsymbol{L} \cdot \boldsymbol{a})^{-1}$, where $\boldsymbol{a} = \boldsymbol{\alpha}/\varepsilon_0 v$, with $\boldsymbol{\alpha}$ the molecular polarizability and v the molecular volume. The linear

TABLE 1. Lorentz-factor tensor components L_{ij} as a function of molecular tilt θ

$\theta(^\circ)$	L_{xx}	L_{xz}	L_{yy}	L_{zz}
0	0.7885	0	0.7885	−0.5769
10	0.7749	−0.0052	0.7851	−0.5603
20	0.7277	−0.0193	0.7834	−0.5112
30	0.6299	−0.0316	0.8126	−0.4425
40	0.4574	−0.0018	0.9670	−0.4244

TABLE 2. Quadratic susceptibility components $\chi_{ijk}/10^{-9}$ esu as a function of molecular tilt θ

$\theta(^\circ)$	χ_{xxx}	χ_{xxy}	χ_{xzz}	χ_{yzz}	χ_{zxx}	χ_{zyx}	χ_{zzz}
0	0	0	6.0	5.5	0	0	−17.7
10	1.5	0.4	9.8	5.6	− 4.1	−1.5	−15.9
20	7.0	1.6	13.1	5.7	−10.0	−3.1	−13.8
30	17.0	3.7	14.6	5.7	−16.4	−4.6	−10.8
40	32.5	6.1	13.0	4.7	−21.6	−5.4	− 6.3

susceptibility $\chi^{(1)}$ (whence the refractive indices) is given by $\boldsymbol{a} \cdot \boldsymbol{d}$. We take the molecular polarizability to have components $(\alpha, \alpha, s\alpha)$ in molecular axes, giving a polarizability per unti volume essentially independent of s for large s. With $\alpha/\epsilon_0 v = 1.5$ we find that x and z remain the principal axes since L_{xz} is so small. As the molecules tilt towards x and away from z, n_x increases from 1.07 to 1.19 at 40° tilt, where n_z decreases from 1.22 to 1.17; n_y remains essentially constant at 1.07.

The quadratic susceptibility $\chi^{(2)}$ is given by $\mathbf{d}^{\mathrm{T}} \cdot \mathbf{b} : \mathbf{dd}$, where $\mathbf{b} = \boldsymbol{\beta}/\epsilon_0 v$ with $\boldsymbol{\beta}$ the molecular hyperpolarizability. We take the molecular hyperpolarizability to be essentially one-dimensional along the molecular axis L, with nonzero components of the form $\beta_{ALL} = (\beta, \beta, -s\beta)$ in molecular axes $A = L, M, N$, a form suggested by MO calculations on NLO molecules. With $\beta/\epsilon_0 v = 1.87 \times 10^{-30}$ esu we find the results for χ_{ijk} as a function of tilt θ shown in Table 2, excluding yyx, yyy and yyz components which never exceed 0.1×10^{-9} esu. Tilt greatly modifies the pattern of components, so that for example even at 20° the xzz component almost equals the zzz component in magnitude, with the zxx component not much smaller. Presumably effects of this sort correspond to the noncentrosymmetry in the plane indicated by the SHG measurements.

Acknowledgments

This work was supported in part by the Ministry of Defence Royal Armaments Research and Development Establishment and by the United States Army through its European Research Office.

References

1 P. Kerkoc, M. Zgonik, K. Sutter, Ch. Bosshard and P. Günter, *J. Opt. Soc. Am. B*, *7* (1990) 313.
2 J. L. Oudar and R. Hierle, *J. Appl. Phys.*, *48* (1977) 2699.
3 J. Zyss, D. S. Chemla and J. F. Nicoud, *J. Chem. Phys.*, *74* (1981) 4800.
4 G. Decher, B. Tieke, Ch. Bosshard and P. Günter, *Ferroelectrics*, *91* (1989) 209.
5 J. P. Bareman and M. L. Klein, *J. Phys. Chem.*, *94* (1990) 5202.
6 M. A. Moller, D. J. Tildesley, K. S. Kim and N. Quirke, *J. Chem. Phys.*, *94* (1992) 8390.
7 M. Bishop and J. H. R. Clarke, *J. Chem. Phys.*, *95* (1991) 540.
8 R. W. Munn, S. E. Mothersdale and M. M. Shabat, in: R. A. Hann and D. Bloor (eds.), *Organic Materials for Nonlinear Optics II*, Royal Society of Chemistry, Cambridge, 1991, p. 34.

DESIGN OF LANGMUIR-BLODGETT FILMS FOR NONLINEAR OPTICS

A. BAGGALEY,[1] M. BISHOP,[1] J.H.R. CLARKE,[1] L.E. DAVIS,[2] T.A. KING,[3] D.A. LEIGH,[1] F.R. MAYERS,[1] A. MOHEBATI,[3] R.W. MUNN,[1] M.M. SHABAT,[1] O. SZCZUR,[1] D. WEST,[3] AND J.O. WILLIAMS[1]

[1]*Department of Chemistry and* [2]*Department of Electrical Engineering and Electronics, UMIST, Manchester M60 1QD, U.K., and* [3]*Department of Physics, University of Manchester, Manchester M13 9PL, U.K.*

Abstract Results are presented on the design, preparation and characterization of Langmuir-Blodgett films formed from stearyl (S) derivatives of DAN, MAP and NPP. Molecular dynamics modelling of trilayers composed of simplified molecules reveals buckling at the interface owing to disordering of the strongly interacting head groups. Model calculations show weak dielectric interactions between neighbouring layers, and reveal major effects of molecular tilt on the quadratic and cubic susceptibilities. SDAN forms good films but SNPP and SMAP do not form stable films even in mixtures with stearic or behenic acid. All three materials give SHG as powders and as LB films. The film SHG coefficients are some 10% of those for crystals of the underivatized molecules.

1. INTRODUCTION

Various organic molecules such as 4-*N*,*N*-dimethylamino-3-acetamidonitrobenzene (DAN, 1), 2,4-dinitrophenyl-1-alanine methyl ester (MAP, 2) and (*S*)-*N*-(4-nitrophenyl)-prolinol (NPP, 3) are known to give crystals with high nonlinear optical response. However, crystal growth is time-consuming and imposes constraints on the possible molecular packings and lattice symmetries. Since these molecules already possess potentially hydrophilic groups, we have adopted the strategy of derivatizing them with hydrophobic stearyl chains to produce SDAN (4), SMAP (5) and SNPP (6).

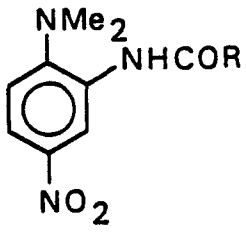

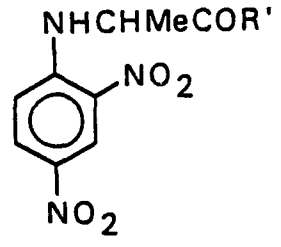

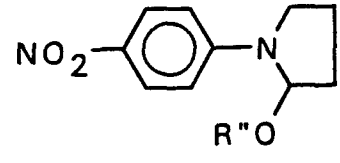

1: DAN, R = CH_3 **2**: MAP, R′ = CH_3 **3**: NPP, R″ = H
4: SDAN, R = $C_{17}H_{35}$ **5**: SMAP, R′ = $C_{18}H_{37}O$ **6**: SNPP, R″ = $C_{17}H_{35}CO$

The aim is to deposit the derivatives as Langmuir-Blodgett films to retain the high molecular response while affording more control of the material structure.

Our approach has four strands: (i) dynamic modelling of films; (ii) calculation of optical properties; (iii) synthesis of film-forming molecules and deposition of films; and (iv) linear and nonlinear optical characterization of films.

2. MOLECULAR DYNAMICS SIMULATIONS

The general aim of the simulations is to understand how interactions between molecules control the structure of multilayer LB films. Modelling has been used to characterize the two types of interface, between chain heads and between the hydrophobic chain ends. We have examined structural correlations between the layers and also the influence of structural defects of the trilayer structure.

Our approach is to use a simplified but computationally tractable model for the amphiphiles which reflects the essential molecular features, i.e. connectivity, van der Waals interactions, and a realistic representation of chain flexibility. In this initial study the chemically complex head groups are represented by a large single interaction site with parameters chosen to reflect the bulkiness and intensity of the associated interactions. The amphiphiles consist of 18 sites linearly connected by rigid bonds (head group plus 16 methylene groups and one terminal methyl group). Lennard-Jones 12 - 6 potentials are used throughout with a cut-off of 3.0 (in units of the appropriate σ). The parameters for the head group interactions are ϵ_h/k_B = 500 K (k_B is the Boltzmann constant), σ_h = 4.611 nm, and m_h = 0.100 kg mol^{-1}, and for the tail are ϵ_t/k_B = 72 K and σ_t = 0.3923 nm. The usual Berthelot combining rules are used for cross interactions. Interactions with the flat, structureless surface are modelled using a 9 - 3 potential with the same parameters as used previously:[1] ϵ_{BS}/k_B = 90 K and σ_{BS} = 0.36 nm, except that the head groups are attracted by a stronger potential ϵ_{HS}/k_B = 302.132 K. No cut-off is used for the surface potential.

The method of preparation is to build and equilibrate the film layer by layer with the heads of the first layer pointing towards the surface. Each layer contains 64 chains for a total of 3456 particles. The chain heads are initially arranged in a hexagonal lattice with the rest of the molecule normal to the surface plane and in the all-trans state. The surface area per head group is 23.2 Å^2/chain. Periodic boundary conditions are imposed in the X and Y directions and the minimum image convention is employed. The first 16,000 time steps (40 ps) are discarded for equilibration.[1] The data are obtained from 100 ps equilibrium simulations.

The tilt angle θ is determined from the angle between the surface normal and the vector between the fourth and fifteenth beads. At 300 K its mean value in the first layer (closest to the surface), $<\theta_1>$ = 39°, is as expected from the simple constant projected area model.[2] The smaller values of $<\theta_2>$ = 35° and $<\theta_3>$ = 31° in the second and third layers indicate that each layer is successively more disordered, a trend reflected in the density of units normal to the surface plane $G(Z)$ presented in Figure 1. The first layer is highly ordered with a sharp first peak corresponding to the head groups. Indeed, seventeen separate peaks corresponding to the tail groups can be resolved. The second and third layers are less ordered although the head peaks are still quite distinct. The radial distribution function projected on to the surface plane $G(R)$ shows that the heads in the first layer are held tightly in the hexagonal lattice structure

whereas those in the second and third layers show almost liquid-like disorder.

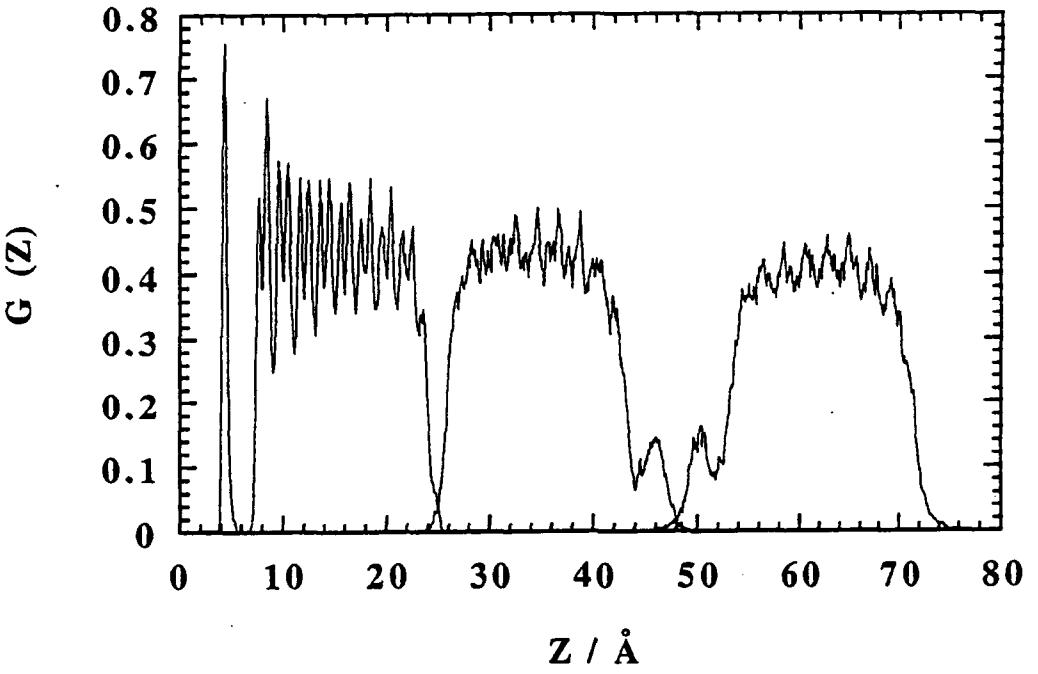

FIGURE 1. Density profile $G(Z)$ in the Z direction normal to the LB film.

The disordering of the strongly interacting head groups can be related to the metastability of the layer structure which results in spontaneous buckling of the interface. This underlines the importance of incorporating orientation-dependent head group interactions in order to stabilize the interfaces better. Some indication of the extent of buckling is given by the difference in half widths of the head group peaks in $G(Z)$ for the second and third layers as compared to the first layer. The value of 0.2 - 0.3 nm is similar in magnitude to that observed experimentally for LB films by atomic force microscopy.[3]

3. CALCULATION OF FILM PROPERTIES

Linear and nonlinear optical response have been calculated for model film structures. The molecules are represented as a string of spherical beads to model their size, shape and orientation, the number of beads giving the axial ratio of the molecule. The long axes are initially packed in a triangular array normal to the layers, but are allowed to tilt by an angle θ along the nearest-neighbour direction, as suggested by the molecular dynamics calculations. The initial structure is hexagonal and becomes monoclinic once the molecules tilt.

The optical properties are determined by the molecular properties, transformed to the film axis system, and by the local polarizing electric fields in the layers. The local fields depend on the planewise Lorentz-factor tensors $L(g)$, which are sums of dipole interactions between a molecule in layer 0 and the molecules in layer g.[4] Components of $L(0)$ (calculated for an axial ratio of 5) referred to monoclinic $x\ y\ z$

axes, with z normal to the layers and xz the plane of tilt, are shown in Table I.

Table I. Planewise sum components $L_{\alpha\beta}(0)$ for various tilts θ.

θ	$\alpha\beta$			
	xx	*xz*	*yy*	*zz*
0°	0.491	0	0.491	-0.982
20°	0.440	0.093	0.467	-0.907
40°	0.281	0.148	0.420	-0.701

At zero tilt the values approach (0.5, 0.5, 0), which is the depolarization factor for a needle-shaped Lorentz cavity appropriate to elongated molecules. (Results reported previously[5] contained a numerical error.) Tilt about *y* affects L_{yy} little, but induces a nonzero L_{xz} and brings L_{xx} and L_{zz} closer. For $g = 1$, the values are at most 1% of the corresponding ones in Table I, and so can be neglected in practice.

Optical properties are calculated using a model molecular polarizability α and first and second hyperpolarizabilities β and γ having the same axial ratio as the molecules. The local field factors are 1.0 to 1.2, with no strong dependence on tilt. Of the refractive indices, n_y varies little, while n_x increases and n_z decreases with increasing tilt, reflecting the variation of the polarizability with tilt. Both quadratic and cubic nonlinear susceptibilities have been calculated, with results as summarized in Tables II and III.

Table II. Quadratic susceptibility components $\chi_{\alpha\beta\gamma}$/pm V^{-1} for various tilts θ.

θ	$\alpha\beta\gamma$					
	xxx	*xxz*	*xyy*	*xzz*	*zyy*	*zzz*
0°	0	4.9	0	0	4.9	-20.9
20°	-3.8	0.2	-1.8	10.7	4.8	-18.5
40°	0.3	-8.8	-3.2	13.5	4.2	-8.3

Table III. Cubic susceptibility components $\chi_{\alpha\beta\gamma\delta}$/(pm V^{-1})^2 for various tilts θ.

θ	$\alpha\beta\gamma\delta$				
	xxxx	*xxxz*	*xxzz*	*xzzz*	*zzzz*
0°	0	0	0	0	11 000
20°	300	-800	1900	-5000	13 400
40°	3400	-4500	5900	-7800	10 300

The pattern of components varies significantly with tilt. This reflects predominantly the effect of tilt on the hyperpolarizability components. The component χ_{xxx} does not depend monotonically on θ because β_{xxx} changes sign as θ increases, and nor does χ_{zzzz} because the direct and cascading contributions (which depend on γ and β^2 respectively[7]) have opposite dependences on θ. The cascading term can be as large as the direct one, and hence should not be ignored in predicting the cubic susceptibility.

4. SYNTHESIS AND FILM DEPOSITION

SDAN (**4**) is synthesized from 1-fluoro-5-nitroaniline by (i) nucleophilic displacement of fluoride in ethanol followed by (ii) amidation with stearic acid, dicyclohexylcarbodiimide and catalytic 4-pyrrolidinopyridine in dichloromethane.[7] SMAP (**5**) is prepared similarly from 2,4-dinitro-fluorobenzene by (i) reaction with D-alanine in ethanol followed by (ii) esterification with stearyl alcohol. SNPP (**6**) presents more difficulty, but can be prepared by (i) amination of 4-fluoro-nitrobenzene with D-proline in ethanol followed by (ii) esterification with stearic acid. All three materials are crystalline solids at room temperature and give satisfactory NMR, IR and microanalytical data after purification by column chromatography on silica gel.

Dipping experiments are carried out using a Joyce-Loebl dual A-B trough. Well-ordered homogeneous non-centrosymmetric multilayers of SDAN are deposited onto silanized glass plates, but dipping films for SMAP and SNPP proves more difficult and less reliable. The films are typically Y-type for SMAP and SNPP and X-type for SDAN, though both Y and Z-type films can also be obtained for SDAN by careful control of the experimental conditions. The films are characterized by X-ray diffraction, UV/visible spectroscopy and optical measurements, which together clearly show tilt angles ranging from near zero to ~30°, depending on the dipping temperature and the pH of the subphase.

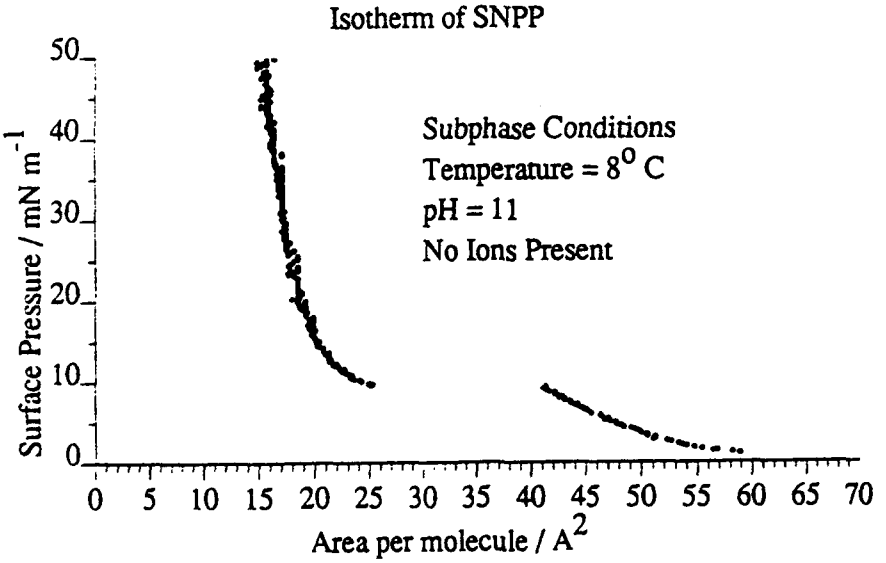

FIGURE 2. Surface isotherm for SNPP indicating monolayer formation.

The highly capricious nature of the films formed by pure SMAP and SNPP led us to investigate their film-forming properties more closely. Systematic variation of temperature and pH gives some isotherms (e.g at 8 °C and pH 11: Figure 2) that indicate the formation of a floating monolayer for SNPP, but no conditions could be found that would allow routine successful dipping of films; the monolayer seems to collapse over a period of about 20 minutes at reasonable dipping pressures. Equimolar mixtures of SNPP with stearic acid or behenic acid (which sometimes stabilize films) deposit better, but give areas per molecule suggestive of the fatty acid alone, a conclusion supported by the observation of SNPP crystallites apparently squeezed out of the film. For SMAP, no conditions are found that give a floating monolayer. Equimolar mixtures with behenic acid give the same sort of behaviour as for SNPP, indicating expulsion of SMAP from the floating monolayer.

The differences in behaviour of these three *p*-nitroaniline derivatives suggest that the position of attachment of the long alkyl chain to the head group controls the conformation and arrangement of the molecules in a manner that is critical for LB film formation. We are currently investigating how to improve the stability and reproducibility of the films by methods including (i) varying the position of attachment of the tails to the NLO-active head groups, (ii) using multiple tails, and (iii) organising the head groups through specific directional and recognitive interactions.

5. FILM CHARACTERIZATION

Second-harmonic generation (Figure 3) is a sensitive probe of structure within the LB nonlinear optical films. A Nd:YAG laser is used which emits Q-switched pulses of 1 mJ energy in 10 ns at a wavelength of 1064 nm with a repetition rate of 30 Hz. The pulses have a Gaussian spatial profile, with stability of the order of 1%. The light is p-polarized and focused onto the sample with a spot size of 300 micron. The angle of incidence onto the sample is stepper-motor controlled. After passage through an infrared-blocking KG3 low pass filter, neutral density filters as required and a 1 nm bandwidth interference filter for the second harmonic at 532 nm, the harmonic signal is detected by a photomultiplier. A boxcar integrator is used to gate the detection system and reduce noise.

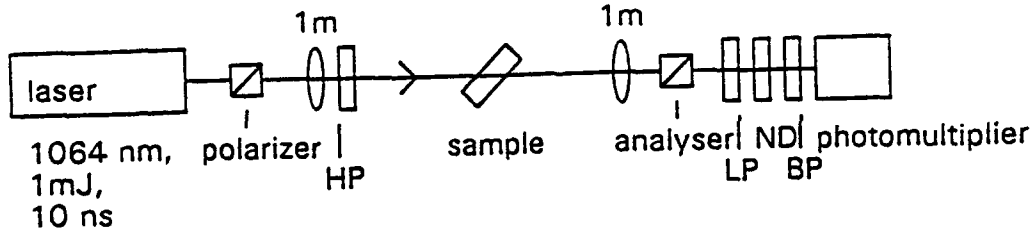

FIGURE 3. Experimental arrangement for studying SHG.

The powders of SDAN, SMAP and SNPP still exhibit SHG, and so the stearyl group does not promote centrosymmetry, in contrast to some results for other *p*-nitroaniline derivatives. The LB films of SDAN, SMAP and SNPP also exhibit SHG. However, since SDAN produces the best films, it has been the subject of the major part of this study. The dependence of SHG on the angle of incidence onto an LB film can be analysed to find the orientation of the nonlinear chromophores within the layers.

SHG results for transmission through an SDAN film coated on both sides of the substrate are shown in Figure 4. The interference between the second harmonic produced at the two surfaces creates fringes with varying angle of incidence. The significant harmonic signal at normal incidence indicates non-centrosymmetric molecular packing in the plane of the film, and the angular dependence of the SHG efficiency indicates that the nonlinear chromophores lie precisely in the plane of the film at the interface of each layer. The nonlinear axis of the SDAN molecule is not parallel to the molecular axis defined by the hydrocarbon chain. The measured intensity does not vary across the film perpendicular to the dipping direction, or along the film parallel to it, to within the accuracy of the measurements.

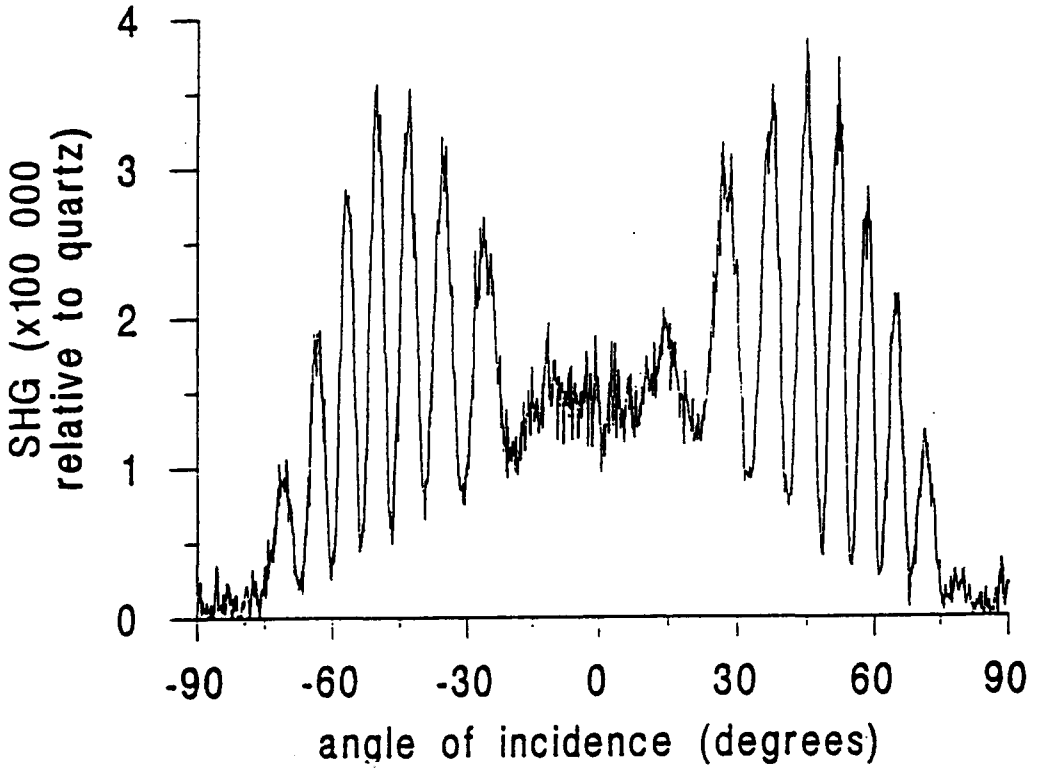

FIGURE 4. Interference fringes from SHG in an SDAN LB film.

LB films of SDAN deposited on a single trough exhibit SHG at normal incidence similar to the material DCANP,[8] also a derivative of *p*-nitroaniline. The nonlinear coefficient of SDAN is $d = 7 \times 10^{-9}$ esu, very similar to the value of 8×10^{-9} esu reported for DCANP. For SDAN the SHG coefficient is about 10% of that of the DAN crystal, without the stearyl chain. For SNPP the coefficient relative to NPP is slightly greater than 10%. Preliminary measurements on SMAP have shown high SHG conversion efficiencies, but with evidence of microcrystallite formation.

The films of SDAN have a very high optical damage threshold, in excess of 1 GW cm^{-2}. They have excellent environmental stability, with no detectable deterioration of nonlinear response after over a year of storage at room temperature including exposure to fluorescent lighting. Systematic study of the film quality as a function of

deposition conditions has not yet allowed the construction of multilayer stacks over 50 layers thick. The films have a slightly milky appearance due to the formation of Rayleigh scatter domains within the film structure. Waveguiding experiments have therefore not yet been possible.

6. CONCLUSIONS

Molecular dynamics simulations provide insight into the structure and perfection of LB films and how these relate to the molecular structure. Model calculations show how the molecular nonlinear response expresses itself in the films, with particular reference to the effect of tilt. Molecules that produce SHG-active crystals have been derivatized to produce LB films, though these are not always stable. The films have SHG coefficients that are 10% of those for the crystals, with good damage resistance and environmental stability.

Current work is aimed at studying in more detail how molecular structure affects film NLO response, in order to improve molecular design, and at designing and synthesizing new species to give uniform thick multilayer films with better optical performance.

ACKNOWLEDGEMENTS

This work was supported by DARPA grant DAJA-49-89-C-0036 and MOD grants 2044/170 and 171.

REFERENCES

1. M. Bishop and J.H.R. Clarke, *J. Chem. Phys.*, **95**, 540 (1991).
2. J.P. Bareman and M.L. Klein, *J. Phys. Chem.*, **94**, 5202 (1990).
3. J. Garnaes, D.K. Schwartz, R. Viswanathan and J.A.N. Zasadrinski, *Nature*, **357**, 54 (1992).
4. R.W. Munn, *J. Chem. Phys.*, in press (15 September 1992).
5. M. Bishop, J.H.R. Clarke, L.E. Davis, T.A. King, F.R. Mayers, A. Mohebati, R.W. Munn, M.M. Shabat, D. West and J.O. Williams, *Thin Solid Films*, **210/211**, 185 (1992).
6. M. Hurst and R.W. Munn, *J. Molec. Electron.*, **2**, 35 (1986).
7. F.R. Mayers, J.O. Williams, A. Mohebati, D. West, T.A. King and G.S. Bahra, in *Organic Materials for Non-Linear Optics II*, edited by R.A. Hann and D. Bloor, RSC Special Publication No. **91** (Royal Society of Chemistry, Cambridge, 1991), p. 96.
8. Ch. Bosshard, G. Decher, B. Tieke and P. Günter, *Proc. SPIE*, **1017**, 141 (1988).

System size dependence and time convergence in molecular dynamics simulations of monolayer films

Marvin Bishop[a] and Julian H. R. Clarke
Department of Chemistry, University of Manchester Institute of Science and Technology, Manchester M60 1QD, England

(Received 24 January 1991; accepted 25 March 1991)

The sample size dependence and time convergence of property values of simple hydrocarbon monolayers has been investigated by performing molecular dynamics simulations at four surface coverages for systems ranging in size from 16 to 100 chains and for trajectories as long as 200 ps. Detailed studies of the tilt angle indicate that systems with 64 chains simulated for 40 ps (in addition to a 40 ps equilibration stage) are large enough to obtain statistically meaningful results. The equilibrium tilt angle is slightly sensitive to the boundary conditions.

The investigation of the structure of Langmuir and Langmuir–Blodgett films has now become an extremely active area of research[1] driven by potential applications in the fabrication of electronic and electro-optic devices. Langmuir films are molecular monolayers at the liquid–gas interface (usually water–air) whereas Langmuir–Blodgett films are mono or multilayer films deposited from the liquid–air interface onto a solid substrate such as silver-plated mica. In order to form a Langmuir film a molecule must be amphiphilic so that its hydrophilic "head" is immersed into the water phase while its hydrophobic tail points into the gas phase. The classic materials used to make Langmuir films are the fatty acids such as arachidic acid, $CH_3(CH_2)_{18}CO_2H$, and its metal salts.

Several simulations of idealized monolayers have been reported in recent years.[2–7] Each research group has, however, used a different molecular model, making it difficult to compare results and to judge the correctness of the conclusions. In order to assess the influence of sample size, initial lattice type and the convergence of property values with time we have carried out a systematic examination of one of these published models[3,4,6] for $N = 20$ unit hydrocarbon monolayers.

In this "united atom" model the hydrogens are collapsed into the carbons so that, for example, a methyl group is replaced by a spherical bead of mass 0.015 kg mol^{-1} and a methylene group by a spherical bead of mass 0.014 kg mol^{-1}. The connectivity of the chains is maintained by joining the interaction sites by N-1 rigid bonds (kept at a constant magnitude of 0.153 nm, with a relative tolerance of 10^{-6}, by the SHAKE[8,9] procedure for constraint dynamics).

Each chain has N-2 bond angles, θ_i, which are subject to the following harmonic potential

$$U(\theta_i) = 0.5k_\theta(\theta_i - \theta_0)^2. \quad (1)$$

Here, k_θ and θ_0 are the equilibrium bond angle force constant and bond angle, respectively. These have the values[10] $k_\theta = 520$ kJ mol^{-1} rad^{-2} and $\theta_0 = 109.47°$. A torsional potential $U(\alpha)$ for the dihedral angle α between the two planes formed by four consecutive chain units is included.[11]

$$U(\alpha) = c_0 + c_1\cos(\alpha) + c_2\cos^2(\alpha) + c_3\cos^3(\alpha) + c_4\cos^4(\alpha) + c_5\cos^5(\alpha), \quad (2)$$

where c_0, c_1, c_2, c_3, c_4, and c_5 have the values 9.2789, 12.1557, −13.1201, −3.0597, 26.2403, and −31.4950 in units of kJ mol^{-1}, respectively.

In addition to the above potential interactions all pairs of units on a given chain which are separated by at least four bonds and all pairs on different chains interact through a Lennard-Jones 12–6 potential which is truncated[6] at 2.294 σ. The values for the Lennard-Jones constants[6] are $\epsilon/k_b = 72$ K (k_b is Boltzmanns' constant) and $\sigma = 0.3923$ nm.

In the model[3,4,6] all of the units interact with a flat, structureless surface (set at $Z = 0$) by a functional form of the Lennard-Jones potential which results from integration over the surface[12] (viz. 9–3 instead of the usual 12–6).

$$U_{BS} = 20\epsilon_{BS}[(\sigma_{BS}/Z)^9 - (\sigma_{BS}/Z)^3]. \quad (3)$$

We have selected the same set of parameter values as employed by Bareman and Klein[6] $\epsilon_{BS}/k_b = 90$ K and $\sigma_{BS} = 0.36$ nm. No cutoff is used for the surface potential.

The systems initially have their chain "heads" arranged in either a triangular or a square lattice with the rest of the molecule normal to the $Z = 0$ plane and in the all trans state. The Verlet algorithm[13] with a time step of 2.5 fs was used to integrate Newton's equations of motion. Periodic boundary conditions were imposed in the X and Y directions and the minimum image convention was employed. Following Bareman *et al.*[4] the first 16 000 time steps (40 ps) have been discarded for equilibration. Molecular dynamics simulations for 80 ps on a single processor of a Silicon Graphics 260 GTX require about four days of computer time for 64 chain systems.

The surface coverage is conveniently defined by the area per chain A_c. We have carried out simulations at A_c values of 19.6, 20.8, 22.0, and 23.2 Å^2/chain for sample sizes N_c ranging from 16 to 100 chains. For the two largest values of A_c we have used 200 ps simulations which appear to be ten times

[a] Permanent address: Department of Mathematics/Computer Science, Manhattan College, Riverdale, New York 10471.

 0021-9606/91/130540-04$03.00

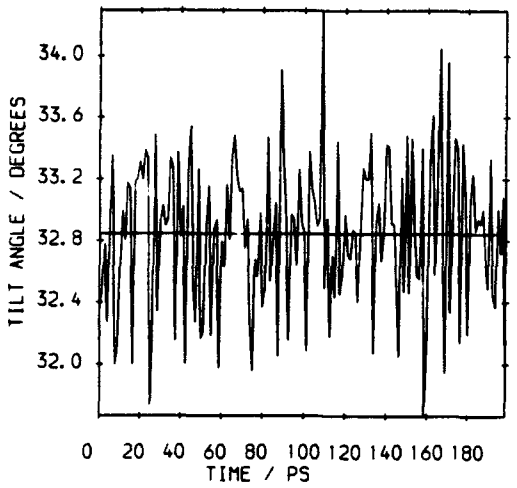

FIG. 1. The time variation of the tilt angle for a 64 chain system with $A_c = 22.0$ Å^2/chain. The horizontal line is the final average.

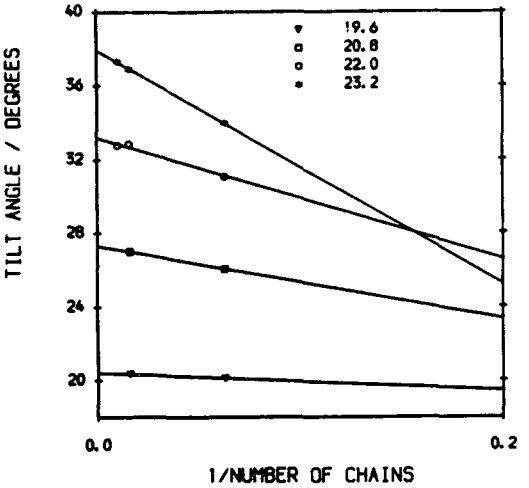

FIG. 2. The extrapolation of the tilt angle for different areas per chain for the triangular lattice.

longer than those reported by Bareman *et al.*[4] The main quantities which have been monitored are the temperature $\langle T \rangle$, the various energies (bond angle $\langle EB \rangle$, torsional $\langle ET \rangle$, Lennard-Jones $\langle ELJ \rangle$, surface $\langle ES \rangle$, and total potential energy $\langle EP \rangle$), the percentage of trans states (conformations with $|\alpha| < 60°$) $\langle \%T \rangle$, and the tilt angle from the normal direction $\langle \beta \rangle$. The tilt angle has been determined from the angle the vector between the fourth and seventeenth beads makes with the normal direction.[6] The chain ends are not used in the calculation of the tilt angle since the probability for gauche configurations at the ends can be quite high.[3-7,14] The angular brackets indicate that the value of the system property is time averaged over the equilibrated molecular dynamics trajectory. The variation of tilt angle with time is shown in Fig. 1 for the 200 ps following the initial 40 ps equilibration phase in a 64 chain system with $A_c = 22.0$ Å^2/chain. This figure suggests that the value of 32.85 indicated by the horizontal line is close to the equilibrium average.

TABLE I. The simulation results starting with a triangular lattice.

	$A_c = 19.6$ (20 ps)		
	16	64	
$\langle T \rangle$/K	302.31 ± 0.95	300.30 ± 0.45	
$\langle ELJ \rangle$/kJ mol^{-1}	− 158.80 ± 0.11	− 159.17 ± 0.04	
$\langle ES \rangle$/kJ mol^{-1}	− 17.09 ± 0.33	− 16.70 ± 0.02	
$\langle \%T \rangle$	99.43 ± 0.32	99.39 ± 0.02	
$\langle \beta \rangle$/deg	20.11 ± 0.12	20.34 ± 0.04	
	$A_c = 20.8$ (20 ps)		
	16	64	
$\langle T \rangle$/K	301.63 ± 0.97	297.75 ± 0.50	
$\langle ELJ \rangle$/kJ mol^{-1}	− 154.88 ± 0.11	− 156.66 ± 0.06	
$\langle ES \rangle$/kJ mol^{-1}	− 17.79 ± 0.05	− 17.59 ± 0.02	
$\langle \%T \rangle$	98.05 ± 0.08	98.82 ± 0.02	
$\langle \beta \rangle$/deg	26.06 ± 0.09	26.99 ± 0.05	
	$A_c = 22.0$ (200 ps)		
	16	64	100
$\langle T \rangle$/K	306.66 ± 1.05	310.09 ± 0.53	306.25 ± 0.36
$\langle ELJ \rangle$/kJ mol^{-1}	− 152.69 ± 0.12	− 155.06 ± 0.05	− 155.05 ± 0.04
$\langle ES \rangle$/kJ mol^{-1}	− 18.58 ± 0.04	− 18.91 ± 0.02	− 18.86 ± 0.02
$\langle \%T \rangle$	98.32 ± 0.06	98.44 ± 0.03	98.49 ± 0.02
$\langle \beta \rangle$/deg	31.05 ± 0.08	32.85 ± 0.04	32.78 ± 0.03
	$A_c = 23.2$ (200 ps)		
	16	64	100
$\langle T \rangle$/K	302.61 ± 1.06	300.39 ± 0.54	305.83 ± 0.41
$\langle ELJ \rangle$/kJ mol^{-1}	− 147.47 ± 0.12	− 153.29 ± 0.06	− 153.85 ± 0.04
$\langle ES \rangle$/kJ mol^{-1}	− 19.33 ± 0.05	− 19.90 ± 0.02	− 20.01 ± 0.02
$\langle \%T \rangle$	97.12 ± 0.09	98.28 ± 0.04	98.36 ± 0.03
$\langle \beta \rangle$/deg	33.96 ± 0.08	36.89 ± 0.04	37.31 ± 0.04

The simulation results for the triangular lattice are presented in Table I. The errors indicated are one standard deviation of the mean. Data were gathered at intervals which are much larger than the correlation time so that it is sufficient to use statistical methods for independent quantities.[15] The error bars on the larger chain system values are smaller than those for the smaller chain values as is expected from statistical considerations. For all of the results with 16 chains the range of the potential in the smaller of the cell dimensions is slightly less than the Lennard-Jones cutoff; we do not expect this to have a strong influence on the observed properties.

The results show that 16, 64, and 100 chain systems display approximately the same energy values per mole. The internal chain energies such as the bond angle energy and the torsional energy are hardly affected by the change in A_c but the Lennard-Jones energy becomes less negative and the surface energy becomes more negative as A_c increases. These

TABLE II. The tilt angle at different areas per chain.

	Extrapolation	Eq. (4)	Bareman and Klein (Ref. 6)
19.6 Å^2/chain	20.42 ± 0.07	19.98	≈20
20.8 Å^2/chain	27.30 ± 0.07	27.68	≈27
22.0 Å^2/chain	33.20 ± 0.03	33.15	≈31
23.2 Å^2/chain	37.92 ± 0.04	37.44	

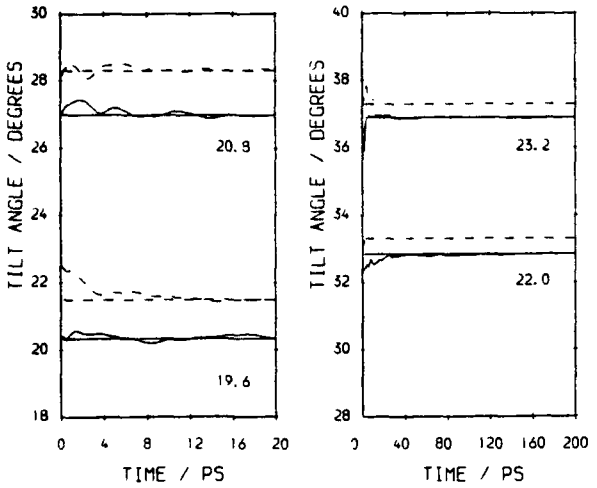

FIG. 3. Time variation of the running average of the tilt angle for different areas per chain; solid line—triangular lattice, broken line—square lattice. The horizontal lines are the final average values.

observations reflect the enhanced influence of the surface as A_c increases. Similarly, the average tilt angle increases as A_c increases because the chains have more room in which to cant over. The percentage of *gauche* states increases slightly from about 1% to 1.5% as A_c increases since more space is now available for *gauche* defects to develop. The percentage of *trans* states found in these molecular dynamics simulations is in good agreement with other workers.[3,6,14]

Since the tilt angle is a crucial property of film systems we have investigated its behavior in more detail. The tilt angle values for finite N_c have been used to obtain the tilt angle values for infinite N_c by fitting a weighted least-squares[16] linear line in $1/N_c$ to each set of data in Table I. The resulting intercepts are 20.42 ± 0.07, 27.30 ± 0.07, 33.20 ± 0.03, and 37.92 ± 0.04 for $A_c = 19.6$, 20.8, 22.0 and 23.2 Å^2/chain, respectively. This extrapolation procedure is illustrated in Fig. 2. The fits at the higher area per chain values indicate that for a small number of chains ($N_c < 7$) the tilt angle of the 23.2 Å^2/chain system will be smaller than that of 22.0 Å^2/chain system. This reflects the large influence of the boundary conditions in small chain systems.

Bareman and Klein[6] suggest that the variation of the tilt angle with A_c is given by

$$\langle \beta \rangle = \cos^{-1}(A_{c0}/A_c), \tag{4}$$

where A_{c0} is the area per chain at maximum thickness (i.e., when all the molecules are normal to the surface). They found for the "united atom" model that $A_{c0} = 18.42$ Å^2/chain. Table II lists the extrapolated molecular dynamics data, the predictions of Eq. (4) and the molecular dynamics results of Bareman and Klein[6] for $N_c = 90$; their values have been read from their Fig. 3. The values predicted by Eq. (4) are in excellent agreement with our extrapolated molecular dynamics data. The value at 22.0 Å^2/chain reported by Bareman and Klein[6] (≈ 31) is significantly lower than that found in this work or predicted by Eq. (4). We suspect that their trajectory was not long enough adequately to sample the tilt angle at this area per chain.

Since the tilt angle results for the 64 chains are in excellent agreement with Bareman and Klein's[6] calculation using 90 chains (at the two lowest areas per chain) and are also in excellent agreement with the 100 chain systems (at the two largest areas per chain) we can conclude that 64 chain systems are large enough to give accurate calculations of the tilt angle.

The convergence of the tilt angle with time is illustrated in Fig. 3 for the 64 chain systems. Even at the highest area per chain of 23.2 Å^2/chain the running average has converged by 40 ps. Thus, it is sufficient to simulate 64 chain systems for 40 ps (in addition to a 40 ps equilibration stage) in order to have good statistics on the tilt angle.

The simulations have been repeated for 64 chain systems starting with the heads initially arranged in a periodic square lattice and the results are contained in Table III. At the two lower densities the runs were performed for 40 ps (in addition to a 40 ps equilibration stage). At the higher densities results from triangular lattice simulations suggest that 20 ps is sufficient to accumulate satisfactory statistics. The convergence of tilt angle with time is included in Fig. 3. It is seen that convergence is achieved for all the areas per chain studied. When one compares Tables I and III one notes that $\langle ES \rangle$ and $\langle \beta \rangle$ for the square lattice is always larger than for the triangular lattice at the same values of A_c (the difference in $\langle \beta \rangle$ increases from about 0.4° to 1.2° as A_c decreases from 23.2 to 19.6 Å^2/chain).

That is at first somewhat surprising since the triangular lattice is the closed-packed arrangement which for a given coverage might be expected to allow more efficient packing of the tails and hence lead to greater tilt. Although the molecules are free to move in the surface plane, for the square lattice simulations they are prevented from taking up a close-packed arrangement by the boundary conditions. Nevertheless enhanced tilt can still be achieved along the diagonals of a square lattice.

The research reported herein has been sponsored in part

TABLE III. The simulation results for a 64 chain system starting with a square lattice.

	19.6 (20 ps)	20.8 (20 ps)	22.0 (40 ps)	23.2 (40 ps)
$\langle T \rangle$/K	303.90 ± 0.55	302.95 ± 0.49	307.83 ± 0.53	302.10 ± 0.54
$\langle ELJ \rangle$/kJ mol^{-1}	-159.31 ± 0.05	-157.86 ± 0.06	-155.77 ± 0.05	-153.21 ± 0.06
$\langle ES \rangle$/kJ mol^{-1}	-16.91 ± 0.02	-18.00 ± 0.02	-19.01 ± 0.02	-19.93 ± 0.02
$\langle \%T \rangle$	99.17 ± 0.02	98.69 ± 0.02	98.82 ± 0.03	98.27 ± 0.03
$\langle \beta \rangle$/deg	21.50 ± 0.04	28.30 ± 0.05	33.31 ± 0.05	37.29 ± 0.04

by the United States Army through its European Research Office and by the Donors of the Petroleum Research Fund, administered by the American Chemical Society. We wish to thank Dr. David Brown for helpful discussions.

[1]See, for example, G. G. Roberts, Adv. Phys. **34**, 475(1985); R. H. Tredgold, Rep. Prog. Phys. **50**, 1609 (1987); V. K. Agarwal, Phys. Today, June, 40 (1988).
[2]A. J. Kox, J. P. J. Michels, and F. W. Wiegel, Nature **287**, 317 (1980).
[3]G. Cardini, J. P. Bareman, and M. L. Klein, Chem. Phys. Lett. **145**, 493 (1988).
[4]J. P. Bareman, G. Cardini, and M. L. Klein, Phys. Rev. Lett. **60**, 2152 (1988).
[5]J. Harris and S. A. Rice, J. Chem. Phys. **89**, 5398 (1988).
[6]J. P. Bareman and M. L. Klein, J. Phys. Chem. **94**, 5202 (1990).
[7]M. A. Moller, D. J. Tildesley, K. S. Kim, and N. Quirke, J. Chem. Phys. (in press).
[8]J. P. Ryckaert, G. Cicotti, and H. J. C. Berendsen, J. Comp. Phys. **23**, 327 (1977).
[9]W. F. van Gunsteren and H. J. C. Berendesen, Mol. Phys. **34**, 1311 (1977).
[10]P. van der Ploeg and H. J. C. Berendsen, J. Chem. Phys. **76**, 3271 (1982).
[11]J. P. Ryckaert and A. Bellemans, Faraday Discuss. Chem. Soc. **66**, 95 (1978).
[12]It has been shown that the replacement of the discrete set of surface sites by a continuum approximation actually yields the result $U_{BS} = (2\pi\rho\epsilon_{BS}\sigma_{BS}^3/3)[2/15\,(\sigma_{BS}/Z)^9 - (\sigma_{BS}/Z)^3]$, where ρ is the number density of the solid surface. See, for example, W. A. Steele, *The Interaction of Gases with Solid Surfaces* (Pergamon, Oxford, 1974).
[13]L. Verlet, Phys. Rev. **159**, 98 (1967).
[14]T. Yamamoto, J. Chem. Phys. **93**, 5990 (1990).
[15]M. Bishop and S. Frinks, J. Chem. Phys. **87**, 3675 (1987), and references therein.
[16]P. R. Bevington, *Data Reduction and Error Analysis for the Physical Sciences* (McGraw-Hill, New York, 1969).

Theory of Non-linear Optical Response in Molecular Layers

R.W. Munn, S.E. Mothersdale, and M.M. Shabat

DEPARTMENT OF CHEMISTRY, UMIST, MANCHESTER M60 1QD, UK

1 INTRODUCTION

Nonlinear optics has provided a useful testing ground for the concept of molecular engineering. One seeks to design and synthesize molecules of high nonlinear optical response, and then to fabricate a molecular material in which this response is effectively expressed. In many such materials the active region is limited in thickness. Obvious examples are Langmuir-Blodgett films[1] and polymer films.[2] Less obvious are molecular crystalline thin films or crystalline cored fibres,[3] or active species diffused into the surface of an optical polymer.[4] Finally, centrosymmetric materials lacking any bulk quadratic nonlinearity may display surface nonlinearity[5] or pyroelectricity.[6]

Molecular theories of nonlinear optical response in thin layers are not well developed. As in theories of bulk nonlinear response, a common approach has been to approximate the local electric field by the Lorentz expression. The Lorentz approximation is known to be poor for crystals of elongated molecules such as p-terphenyl[7] and the polydiacetylenes,[8] so that its reliability is questionable in Langmuir-Blodgett films, at least.

A rigorous treatment of the local field in bulk nonlinear optics of molecular crystals is available, however,[9-11] and has been applied to several species.[12] Molecular theories of linear optical response in thin layers were also developed some 20 years ago in connection with studies of surface excitations. Hence this paper describes a molecular theory of nonlinear optical response in ordered layers, combining the rigour

of the bulk nonlinear theory with the conceptual approach of the thin layer linear theory.

2 LOCAL FIELD

Consider an assembly of layers labelled g = 0,1,.... The layers are assumed to be ordered, and for simplicity to contain only one molecule per two-dimensional unit cell. In a uniform applied electric field $\mathbf{E}^o$, a molecule in layer g experiences a local electric field

$$\mathbf{f}_g = \mathbf{E}^o + \sum_{g'} \mathbf{T}_{gg'} \cdot \mathbf{p}_{g'} / \varepsilon_o v \qquad (1)$$

$$= \mathbf{E}^o + \sum_{g'} \mathbf{T}_{gg'} \cdot \mathbf{a} \cdot \mathbf{f}_{g'}. \qquad (2)$$

Here $\mathbf{T}_{gg'}$ is a dimensionless planewise dipole tensor sum, which gives the field at a molecule in layer g due to the induced dipole moments $\mathbf{p}_{g'}$ in layer g', where g' may equal g; v is the volume per molecule. The induced dipoles are related to the local field by the linear polarizability α, leading to Eq.(2), where $\mathbf{a} = \alpha/\varepsilon_o v$. All layers are treated as equivalent.

Now $\mathbf{T}_{gg'}$ falls off rapidly with the distance between layers g and g'. This allows one to define a range r such that $\mathbf{T}_{gg'}$ is negligible for $|g-g'|>r$, i.e. when r or more layers intervene between g and g'. Then only layers $g'<r$ are coupled to the surface layer g = 0. Furthermore, such layers couple only to further r layers deeper in the assembly. Hence beyond layer 2r, effectively the bulk environment is experienced, and all layers have the same local field. If the assembly is thin enough, there is no bulk region.

For a thin assembly of t layers, Eq. (2) is solved directly by matrix inversion, with the result

$$\mathbf{f}_g = \sum_{g'} (\mathbf{I} - \mathbf{T}\cdot\mathbf{A})^{-1}_{gg'} \cdot \mathbf{E}^o \qquad (3)$$

$$\equiv \sum_{g'} \mathbf{H}_{gg'} \cdot \mathbf{E}^o \equiv \mathbf{h}_g \cdot \mathbf{E}^o. \qquad (4)$$

Here the matrix to be inverted is of dimension 3t x 3t, with 3 x 3 submatrices $\mathbf{1}\delta_{gg'} - \mathbf{T}_{gg'} \cdot \mathbf{a}$. The quantity $\mathbf{h}_g$ is the local-field tensor. This result resembles that for a

molecular crystal[15] but with the label g for a layer replacing the label k for a molecule in the unit cell.

For a thick assembly, some layers experience the bulk environment where the local field becomes $\mathbf{f}^b$, independent of g. Then Eq. (2) becomes

$$\mathbf{f}^b = \mathbf{E}^o + \sum_{g'} \mathbf{T}_{gg'}\cdot\mathbf{a}\cdot\mathbf{f}^b = \mathbf{E}^o + \mathbf{T}^b\cdot\mathbf{a}\cdot\mathbf{f}^b, \qquad (5)$$

where $\mathbf{T}^b$ is the bulk dipole tensor sum

$$\mathbf{T}^b = \sum_{g'} \mathbf{T}_{gg'} \sim \sum_{g'=g-r}^{g+r} \mathbf{T}_{gg'} \ . \qquad (6)$$

It follows that

$$\mathbf{f}^b = (\mathbf{1} - \mathbf{T}^b\cdot\mathbf{a})^{-1}\cdot\mathbf{E}^o \equiv \mathbf{h}^b\cdot\mathbf{E}^o, \qquad (7)$$

with $\mathbf{h}^b$ the bulk local-field tensor.

The surface-induced deviation from the bulk local field $\boldsymbol{\phi}_g = \mathbf{f}^b - \mathbf{f}_g$ follows on subtracting Eq.(5) from Eq. (2), to obtain

$$\boldsymbol{\phi}_g = \sum_{g'} \mathbf{T}_{gg'}\cdot\mathbf{a}\cdot\boldsymbol{\phi}_{g'} + \mathbf{T}_g^s\cdot\mathbf{a}\cdot\mathbf{f}^b. \qquad (8)$$

The quantity $\mathbf{T}_g^s$ is the surface-induced deviation from the bulk dipole sum tensor, given by

$$\mathbf{T}_g^s = \mathbf{T}^b - \sum_{g'} \mathbf{T}_{gg'}. \qquad (9)$$

Comparison with Eq.(6) shows that since $g' \geq 0$, $\mathbf{T}_g^s$ is nonzero for all $g<r$, i.e. for layers within range of the surface. For example, the surface layer g=0 interacts with r other layers on one side only, whereas a bulk layer interacts with r layers on either side. Solution of Eq. (8) gives $\boldsymbol{\phi}_g$, whence

$$\mathbf{f}_g = (\mathbf{1} - \sum_{g'} \mathbf{H}_{gg'}\cdot\mathbf{T}_{g'}^s\cdot\mathbf{a})\cdot\mathbf{h}^b\cdot\mathbf{E}^o \equiv \mathbf{h}_g\cdot\mathbf{E}^o. \qquad (10)$$

Here $\mathbf{H} = (\mathbf{I}-\mathbf{T}\cdot\mathbf{A})^{-1}$ as before, but is now of dimension $3(2r+1) \times 3(2r+1)$, allowing for the full span of non-negligible interactions involving layers 0 to 2r.

3 MACROSCOPIC FIELD

The foregoing provides computable expressions for the linear local field in terms of the applied field $\mathbf{E}^o$ in the absence of the sample. However, experimental quantities such as susceptibilities relate to the macroscopic field in the presence of the sample. Although the applied field is uniform, the material response is not, and hence neither is the macroscopic field.

In layer g the macroscopic field $\mathbf{E}_g$ is given by

$$\mathbf{E}_g = \mathbf{E}^o - \mathbf{n}(\mathbf{n}\cdot\mathbf{p}_g)/\varepsilon_o v, \qquad (11)$$

where $\mathbf{n}$ is a unit vector normal to the layers. The normal component of the polarization in the layer $\mathbf{n}\cdot\mathbf{p}_g/v$ corresponds to a surface charge density σ contributing a field of magnitude σ/ε_o normal to the layers. The combination $\mathbf{p}_g/\varepsilon_o v$ can be related to $\mathbf{E}^o$ or $\mathbf{E}_g$ according to

$$\mathbf{p}_g \ / \ \varepsilon_o v \ = \mathbf{a}\cdot\mathbf{f}_g = \mathbf{a}\cdot\mathbf{h}_g\cdot\mathbf{E}^o \qquad (12)$$

$$= \mathbf{a}\cdot\mathbf{d}_g\cdot\mathbf{E}_g = \chi_g^{(1)}\cdot\mathbf{E}_g \qquad (13)$$

Here $\mathbf{d}_g$ is the usual local-field tensor and $\chi_g^{(1)}$ is the linear susceptibility for layer g. By substituting Eqs (12) and (13) in Eq.(11) one obtains

$$\mathbf{1} + \mathbf{n}(\mathbf{n}\cdot\chi_g^{(1)}) = [\mathbf{1} - \mathbf{n}(\mathbf{n}\cdot\mathbf{a}\cdot\mathbf{h}_g)]^{-1}, \qquad (14)$$

which determines $\chi_g^{(1)}$ and $\mathbf{d}_g$ since $\mathbf{h}_g$ is known from Eq. (10).

Algebraic evaluation of $\chi_g^{(1)}$ is not straightforward because of the unit vector $\mathbf{n}$. By writing

$$\mathbf{T}_{gg'} = \mathbf{L}_{gg'} - \mathbf{nn}\,\delta_{gg'}, \qquad (15)$$

where $\mathbf{L}_{gg'}$ is a planewise Lorentz-factor tensor of unit trace, one obtains

$$\mathbf{T}^b = \mathbf{L}^b - \mathbf{nn}, \tag{16}$$

where $\mathbf{L}^b$ is the bulk Lorentz-factor tensor related to $\mathbf{L}_{gg'}$ as $\mathbf{T}^b$ is to $\mathbf{T}_{gg'}$ by Eq.(6). It is known that $\mathbf{T}^b$ obtained by planewise summation depends on the choice of planes in this way, leaving $\mathbf{L}^b$ independent of the choice.[16] Use of Eq. (15) in Eq. (1) with Eq. (11) yields

$$\mathbf{f}_g = \mathbf{E}_g + \sum_{g'} \mathbf{L}_{gg'} \cdot \mathbf{p}_{g'} / \varepsilon_o v, \tag{17}$$

showing that the $\mathbf{L}_{gg'}$ play the same role in terms of $\mathbf{E}_g$ as the $\mathbf{T}_{gg'}$ do in terms of $\mathbf{E}^o$. Considerable algebra eventually leads to the result

$$\chi_g^{(1)} = \sum_{GG'} (I+k)^{-1}_{gG} \mathbf{K}_{GG'} \Big/ \sum_{g'} (I+k)^{-1}_{gg'}. \tag{18}$$

Here $\mathbf{K} = (\mathbf{A}^{-1} - \mathbf{L})^{-1}$ and I and k are scalar matrices with elements $\delta_{GG'}$ and $\mathbf{n}\cdot\mathbf{K}_{GG'}\cdot\mathbf{n}$ respectively. The local-field tensor $\mathbf{d}_g$ follows at once from Eq. (13).

4 OPTICAL RESPONSE

Nonlinear response can now be treated. At the molecular level, the induced dipole moment in layer g becomes

$$\mathbf{p}_g = \alpha\cdot\mathbf{F}_g + \beta:\mathbf{F}_g\mathbf{F}_g + \delta:\cdot\mathbf{F}_g\mathbf{F}_g\mathbf{F}_g \tag{19}$$

Here $\mathbf{F}_g$ is the local field with nonlinear contributions and β and δ are the first and second hyperpolarizabilities; higher terms are neglected. At the macroscopic level the polarization in layer g becomes

$$\mathbf{P}_g/\varepsilon_o = \chi_g^{(1)}\cdot\mathbf{E}_g + \chi_g^{(2)}:\mathbf{E}_g\mathbf{E}_g + \chi_g^{(3)}:\cdot\mathbf{E}_g\mathbf{E}_g\mathbf{E}_g\ , \tag{20}$$

where $\chi_g^{(n)}$ is the nth order susceptibility and terms beyond cubic are neglected. Since Eq. (17) still applies, substitution from Eq.(19) allows $\mathbf{F}_g$ to be related to $\mathbf{E}_g$. Using $\mathbf{P}_g = \mathbf{p}_g/v$ then yields expressions for the $\chi_g^{(n)}$.

Mathematically this process resembles that for a bulk molecular crystal[11] (as for the local field). The results for the nonlinear susceptibilities are

$$\chi_g^{(2)} = \sum_{g'} \mathbf{b}:\cdot\mathbf{D}_{g'g}\mathbf{d}_{g'}\mathbf{d}_g \tag{21}$$

$$\chi_g^{(3)} = \sum_{g'} [\mathbf{c}::\mathbf{D}_{g'g}\mathbf{d}_{g'}\mathbf{d}_g\mathbf{d}_{g'} + 2\mathbf{b}:\cdot\mathbf{D}_{g'g}\mathbf{d}_{g'}\sum_{g''}(\mathbf{D}\cdot\mathbf{L})_{g'g''}\cdot\mathbf{b}:\mathbf{d}_{g''}\mathbf{d}_{g''}], \tag{22}$$

with $\mathbf{b} = \beta/\varepsilon_o v$, $\mathbf{c} = \delta/\varepsilon_o v$, and $\mathbf{D} = (\mathbf{I}-\mathbf{L}\cdot\mathbf{A})^{-1}$.

The nonlinear susceptibilities for layer g depend not only on the local-field tensor $\mathbf{d}_g$ for that layer but also on those for other layers g', coupled by the partial local field tensor $\mathbf{D}_{g'g}$. Owing to the limited range r of the planewise sums, the evaluation of these expressions is reasonably tractable.

5 DISCUSSION

The present results provide a formal microscopic solution for the linear and nonlinear optical and electrical response in an assembly of ordered layers. Extensions to more than one molecule per two-dimensional cell and to alternating or other layer sequences are readily accommodated. The results incorporate the effect of the variation of the electric field through the surface region without invoking any explicit field-gradient or nonlocal polarizability.[17]

Numerical calculations of the nonlinear response require planewise dipole sums as input. Methods for calculating these sums have been developed and implemented previously.[13,14] In aromatic hydrocarbon crystals, interactions between adjacent layers may be only 1% of those within a layer for point molecules.[14] Our calculations for anthracene treated as three point submolecules show that interactions between adjacent layers may be 30% of those within layer, but fall off rapidly between more remote layers, so that the range r = 1. This short range implies that the surface region is very thin. Experiments at optical wavelengths in

transparent regions will then observe only an average response over the surface region.[17]

ACKNOWLEDGEMENTS

This work is supported by SERC Grant GR/F 42195 and by DARPA contract DAJA45-89-C-0036.

REFERENCES

1. A. Barraud and M. Vandevyver, 'Nonlinear Optical Properties of Organic Molecules and Crystals', eds D.S. Chemla and J. Zyss, Academic, Orlando, 1987, Vol. 1, p.357.
2. D.J. Williams, Ref. 1, Vol. 1, p.405.
3. J. Badan, R. Hierle, A. Perigaud and P. Vidakovic, Ref 1, Vol. 1, p.297.
4. R. Glenn, M.J. Goodwin and C. Trundle, J. Mol. Electron., 1987, 3, 59.
5. Y.R. Shen, Natura, 1989, 337, 519.
6. Yu. P. Piryatinsky, M.V. Kurik and S.V. Zavatsky, J. Mol. Electron., 1989, 5, 99.
7. J.H. Meyling, P.J. Bounds and R.W. Munn, Chem. Phys. Letters, 1977, 51, 234.
8. M. Hurst and R.W. Munn, Chem. Phys., 1988, 127, 1.
9. J.A. Armstrong, N. Bloembergen, J. Ducuing and P.S. Pershan, Phys. Rev., 1962, 127, 1918.
10. G.R. Meredith, B. Buchalter and C. Hanzlik, J. Chem. Phys., 1983, 78, 1533; G.R. Meredith, Proc. SPIE, 1987, 824, 126.
11. M. Hurst and R.W. Munn, J. Mol. Electron., 1986, 2, 35.
12. M. Hurst and R.W. Munn, J. Mol. Electron., 1986, 2, 139; 1987, 3, 75; 'Organic Materials for Nonlinear Optics', RSC Special Publication No. 69, eds R.A. Hann and D. Bloor, Royal Society of Chemistry, London, 1989, p.3; 'Molecular Electronics - Science and Technology', ed A. Aviram, Engineering Foundation, New York, 1990, p.267; M. Hurst, R.W. Munn and J.O. Morley, J. Mol. Electron., 1990, 6, 15.
13. G.D. Mahan and G. Obermair, Phys. Rev., 1969, 183, 834.
14. M.R. Philpott, J. Chem. Phys., 1974, 61, 5306; Chem. Phys. Letters, 1975, 30, 387; Phys. Rev., 1975, B12, 5381.
15. R.W. Munn, Mol. Phys., 1988, 64, 1.
16. P.G. Cummins, D.A. Dunmur, R.W. Munn and R.J. Newham, Acta Cryst., 1976, A32, 847.
17. P. Guyot-Sionnest, W. Chen and Y.R. Shen, Phys. Rev., 1986, B33, 8254.

CALCULATIONS OF NONLINEAR OPTICAL PROPERTIES OF MODEL LANGMUIR-BLODGETT FILMS

R.W. Munn and M.M. Shabat
Department of Chemistry and Centre for Electronic Materials,
UMIST, Manchester M60 1QD, U.K.

ABSTRACT

Calculations have been performed on models of Langmuir-Blodgett LB films to explore how molecular nonlinear response expresses itself in film response. The molecules are treated as a string of s beads initially arranged normal to the film with their long axes forming a close-packed hexagonal array, but they are then allowed to tilt away from the vertical. The molecular polarizability α and first hyperpolarizability β are represented by one-dimensional models in which the axial components are s times the perpendicular ones. Because of the layer structure of the films, the dipolar interactions are calculated as planewise sums between one molecule and all the molecules in a given layer. The sums have been calculated for various values of s as a function of tilt; they are negligible except for interactions of a molecule with its own layer. They have then been used to calculate the local electric field, refractive index and quadratic susceptibility $\chi^{(2)}$ for thin films. The results show that tilt has a major effect on the pattern of components of $\chi^{(2)}$ and hence on measured nonlinear optical behaviour. Such information can be used to help guide the design of molecules to achieve desired film properties.

1. INTRODUCTION

Langmuir-Blodgett films promise a number of advantages for applications in molecular electronics. They are compact and highly ordered, and their thickness and structure can be controlled by depositing the desired number and sequence of monomolecular layers. However, realizing their advantages presents the challenge of designing and synthesizing molecules which impart the requisite optical or electrical activity while affording stable high-quality films.

We are undertaking a coordinated project to develop LB films for nonlinear optics.[1] The overall strategy is to take molecules which give crystals with high NLO activity and to derivatize them so that they give good LB films which retain high NLO activity. Our approach has four strands:

- Molecular dynamics simulations to relate film structure and stability to molecular structure.
- Calculation of film properties from film structure to predict NLO activity.
- Synthesis and deposition of LB films to evaluate molecules and techniques.
- NLO characterization of LB films to assess film performance and device potential.

Eventually the aim is that the strands should operate in this sequence, with each providing feedback to the earlier ones, but this is not yet fully achieved while the individual strands are being developed.

The present paper describes work on the second strand. We have performed calculations on simple models of LB films to explore how molecular response expresses itself in film response. This depends on two factors: the molecular arrangements and the molecular interactions.[2] We therefore first describe our model for film structure. Then we calculate the dipolar interactions within the film. This finally allows us to calculate the film properties, with particular reference to the effect of molecular tilt away from the normal to the film.

2. MODEL

Our model is designed to give the film structure directly from the molecular structure. Molecules which yield LB films are typically elongated, and as such resemble those which yield liquid crystals. The effect of molecular elongation has been examined previously in the context of linear optics of liquid crystals[3] and later in nonlinear optics of molecular crystals.[4] The present model derives from this earlier work.

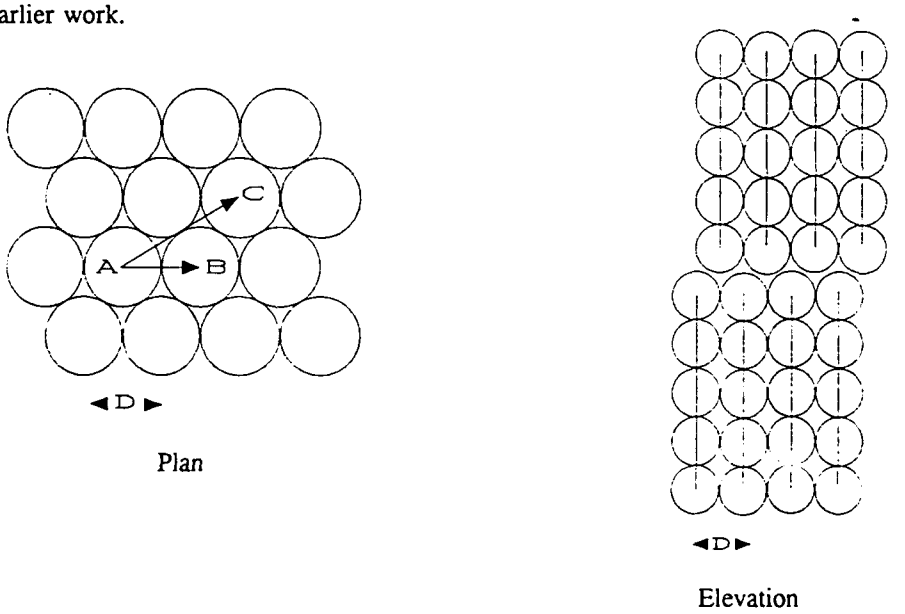

Plan

Elevation

Figure 1. Sketch of the model LB film structure with molecules vertical for $s = 5$.

Each molecule is treated as a string of s spherical "beads", or submolecules. In the basic structure the molecules in each layer form a triangular close-packed arrangement with their long axes normal to the layer. Alternate layers are centred over the triangle formed by the previous layer in such a way that the overall structure has hexagonal symmetry. For simplicity, each layer lies entirely above the preceding

one rather than packing into the recesses of the triangles in the layer below, so that the structure does not reduce to hexagonal close packing for $s = 1$. This structure corresponds to a crystal with lattice parameters $a = b = 2D$, $c = 2sD$, $\alpha = \beta = 90°$ and $\gamma = 120°$, where D is the diameter of a bead. There are two molecules $k = 1, 2$ in the unit cell, with submolecules j located at fractional coordinates $[0, 0, (j - 1)/2s]$ for $k = 1$ and $[1/3, 2/3, 1/2 + (j - 1)/2s)]$ for $k = 2$, where $j = 1,...s$. This structure is illustrated in Figure 1 on the previous page.

Experiments indicate, however, that molecules are typically tilted away from the vertical, and molecular modelling confirms this tendency, explaining it as arising from the attraction of the elongated molecules for the substrate. The resultant structure depends on the plane in which this tilt occurs. All distinct tilted structures are encompassed by tilts in planes lying between the nearest-neighbour direction (AB in Figure 1) and the next-nearest-neighbour direction (AC in Figure 1). The molecular modelling indicates that next-nearest-neighbour tilt is preferred, and we restrict ourselves to such structures.

Now LB films are classified as X, Y or Z-type.[5] X and Z-type films deposit on the substrate only on the upstroke or downstroke of the substrate through the floating Langmuir film, while the commonest (and most stable) Y-type films deposit on both strokes. It is often assumed that Y-type films are centrosymmetric for even numbers of layers and hence cannot exhibit quadratic nonlinearities. This is correct for directions normal to the film, but not for directions parallel to the film when the molecules are tilted.[6] This applies whether the molecules are all tilted in the same sense, to alternate in the direction of tilt, in which case the orthogonal symmetry is retained. (See Figure 2). We consider here only the case of equal tilt θ away from the vertical. The lattice parameters are then $a = b = 2D$, $c = 2D \cos \theta$, $\alpha = \cos^{-1}[(\sqrt{3}/2) \sin \theta]$, $\beta = 90°$, $\gamma = 120°$, with fractional coordinates unchanged.

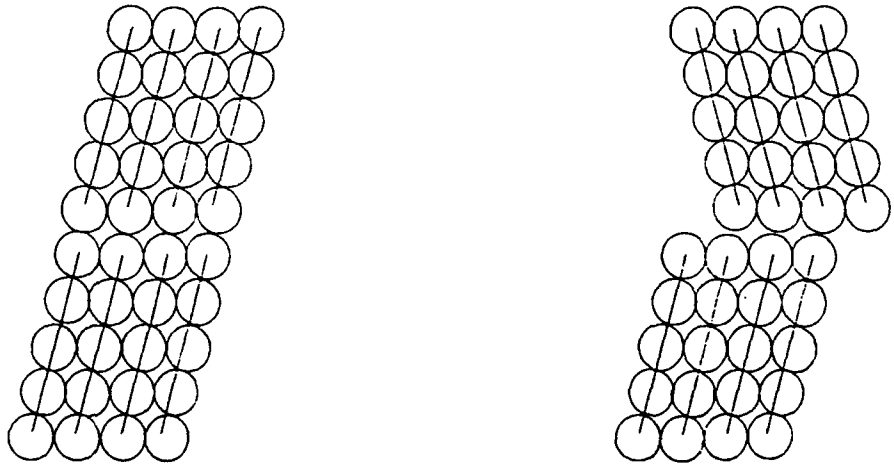

Tilt angles the same Tilt angles alternating

Figure 2. Model LB film structures with molecules tilted for $s = 5$.

We also need a model for the molecular response. Calculations of molecular polarizability and hyperpolarizability as a function of elongation mostly refer to conjugated molecules as opposed to the molecules envisaged here with a conjugated NLO head group and a saturated hydrocarbon tail. For conjugated molecules the axial molecular response is typically found to vary superlinearly with the molecular length. For illustrative purposes we take the axial response in our molecules to be simply proportional to the length. In molecular axes X, Y, Z the polarizability tensor α is then diagonal, with components (α, α, $s\alpha$), and the hyperpolarizability tensor β has non-zero components β_{ZAB} diagonal in AB, with components (β, β, - $s\beta$). Though clearly oversimplified, these assumptions yield an axial molecular response per unit volume which is independent of molecular length, so that changes in susceptibility are directly attributable to changes in structure.

3. PLANEWISE DIPOLE SUMS

Linear and nonlinear response of molecular materials depend on the dipolar interactions in the structure.[7] These relate the local polarizing field at a molecule to the macroscopic electric field E which appears in Maxwell's equations. In a layered structure it is natural to express these interactions as a sum of planewise-dipolar interactions giving the field at a molecule in one layer due to dipoles on the molecules in the same or another layer. calculations for layers of point molecules in aromatic hydrocarbon crystals show that such sums fall off exponentially with distance between the molecule and the layer of dipoles.[8] This gives rise to the idea of a *range* r beyond which the interactions are negligible, so that r defines the number of coupled planes to be included in treating the material properties.[9]

We have calculated planewise sums using standard expressions.[8,10] Sums are calculated between all pairs of submolecules and then averaged to give sums which reflect the molecular size, shape and orientation. For illustrative purposes we report the results for $s = 5$ and explore how the sums depend on the tilt θ. The results, made dimensionless by a factor $v/4\pi$, with v the molecular volume, are given in Table I.

θ	$\alpha\beta$			
	xx	xz	yy	zz
0°	0.491	0	0.491	-0.982
20°	0.429	-0.099	0.456	-0.886
40°	0.284	-0.184	0.412	-0.696

Table I. Planewise dipole tensor sum components $T_{\alpha\beta}(g)$, averaged over submolecules as a function of tilt θ for interactions in the same layer ($g = 0$), expressed relative to cartesian x y z axes, with z the normal to the layers and xz the plane of tilt.

The diagonal components of the planewise dipole sums satisfy Tr $\mathsf{T}(g) = 0$. They are markedly anisotropic, but tilt reduces the anisotropy and induces nonzero components $T_{xz}(g)$, consistent with monoclinic symmetry. For elongated molecules like these, the appropriate Lorentz cavity would be needle shaped, and then we would have the xx components equal to 1/2 and the zz component equal to -1; this is clearly a reasonable approximation to the results for zero tilt. We find that the components for $g = 1$ are much smaller than those for $g = 0$ and so can be neglected (i.e. $r = 1$). Results for values of s up to 10 are very similar. We therefore conclude that the dielectric properties of LB films are dominated by interactions within one layer, with negligible contributions from other layers so that we can drop the label g. In practice much the same result is found for aromatic hydrocarbon crystals, where the bulk properties are dominated by those of a single layer once allowance is made for the slab-shaped crystal implied by the planewise summation.[8]

4. DIELECTRIC RESPONSE

Given the foregoing conclusions, the dielectric response of a film is adequately represented by that of a single layer. The first quantity of interest is the local field $\boldsymbol{F}$. This is related to the applied field by the dipole tensor T, but to the more useful macroscopic field $\boldsymbol{E}$ by the Lorentz-factor tensor $\mathsf{L} = \mathsf{T} + \boldsymbol{nn}$, where $\boldsymbol{n}$ is the unit vector normal to the layers.[11] Then in the present case $L_{\alpha\beta} = T_{\alpha\beta}$ except that $L_{zz} = T_{zz} + 1$, and hence Tr $\mathsf{L} = 1$. We define the local-field tensor by $\boldsymbol{F} = \mathsf{d} \cdot \boldsymbol{E}$, and obtain

$$\mathsf{d} = (1 - \mathsf{L} \cdot \mathsf{a})^{-1}, \tag{1}$$

where $\mathsf{a} = \alpha/\epsilon_0 v$ is a dimensionless reduced polarizability. The calculated local-field components for the reduced bead polarizability $\alpha/\epsilon_0 v = 0.2$ are given in Table II.

θ	$\alpha\beta$								
	xx	xy	xz	yx	yy	yz	zx	zy	zz
0°	1.109	0	0	0	1.109	0	0	0	1.018
20°	1.112	0	0.025	0	1.100	0	0.001	0	1.085
40°	1.085	0	-0.142	0	1.089	0	0.028	0	1.151

Table II. Local-field tensor components $d_{\alpha\beta}$ as a function of tilt expressed relative to the cartesian axes x y z defined in Table I.

The local fields are not greatly different from the macroscopic field. The dependence on tilt is not very marked, and is not monotonic because tilt affects corresponding components of L and a in opposite senses in the xz plane.

The linear susceptibility $\chi^{(1)}$ follows from d as

$$\chi^{(1)} = \mathsf{a} \cdot \mathsf{d} \tag{2}$$

and the relative permittivity is then $\epsilon = \chi^{(1)} + 1$. The refractive indices are obtained from the indicatrix or inverse relative permittivity ϵ^{-1}: for a direction e, the refractive index n_e is given by $1/n_e^2 = e \cdot \epsilon^{-1} \cdot e$. Calculated refractive indices and the angle ϕ between the principal axes of refraction and the x and z axes are given in Table III.

θ	n_x	n_y	n_z	ϕ
0°	1.105	1.105	1.421	0°
20°	1.134	1.096	1.389	9.3°
40°	1.214	1.104	1.281	31.2°

Table III. Refractive indices in the x, y and z directions and the angle between principal axis of refraction and x direction as a function of tilt.

As the molecular long axis tilts away from the vertical z axis and towards the $-x$ axis, n_z decreases and n_x increases as expected, while n_y increases slightly. The angle ϕ, measured from $+x$ towards $+z$, increases with the tilt but lags about 10° behind it, so that the principal axis does not exactly follow the molecular long axis.

The quadratic susceptibility is given by

$$\chi^{(2)} = \mathsf{d}^{\mathsf{T}} \cdot \beta : \mathsf{dd} \,/\, \epsilon_0 v \tag{3}$$

where the superscript T denotes the transpose. Calculated components of $\chi^{(2)}$ are given in Table IV.

θ	$\alpha\beta\gamma$					
	xxx	*xxz*	*xyy*	*xzz*	*zyy*	*zzz*
0°	0	11.8	0	0	11.8	-49.8
20°	-9.2	0.6	-4.3	25.6	11.5	-44.2
40°	0.8	-21.0	-7.6	32.3	10.0	-19.9

Table IV. Quadratic susceptibility components $\chi_{\alpha\beta\gamma}/10^{-9}$ esu as a function of tilt; only independent nonzero components are shown.

The calculated behaviour of χ_{xxx} can be understood in terms of the negative

sign of the ZZZ component of β and the positive sign of the other components, but generally the smaller off-diagonal elements of β enhance the effect of β_{ZZZ}. Tilt induces additional nonzero components of $\chi^{(2)}$, so that at 40° tilt the pattern is very different from that at zero tilt, with χ_{zzz} no longer the largest component in magnitude or even the most negative component. Clearly this would have a significant effect on nonlinear optical measurements.

5. DISCUSSION

The present results show how one can proceed from suitable models of LB film structure and of molecular response to calculate the linear and nonlinear optical properties of the film. The values presented here are illustrative rather than definitive, but they do yield plausible results. The models are simplified, particularly for the distribution of molecular response, which is unlikely to be the same for each "bead" in molecules of practical interest, but more realistic treatments can be carried out when required. As indicated in the Introduction, these calculations can be combined with molecular dynamics modelling to allow one to predict the response of films made from specifically designed molecules, and hence to implement a systematic approach to this area of molecular electronics.

ACKNOWLEDGEMENT

This work was supported by DARPA contract no. DAJA 45-89-C-0036. We thank J.H.R. Clarke, L.E. Davis, T.A. King, D.A. Leigh and J.O. Williams.

REFERENCES

1. M. Bishop, J.H.R. Clarke, L.E. Davis, T.A. King, F.R. Mayers, A. Mohebati, R.W. Munn, M.M. Shabat, D. West and J.O. Williams, Thin Solid Films (LB5 Conference issue), in press.
2. R.W. Munn, in *Molecular Electronics*, ed. P.I. Lazarev (Kluwer, Dordrecht, 1991), p.1.
3. D.A. Dunmur and R.W. Munn, Chem. Phys. **76**, 249 (1983).
4. M. Hurst and R.W. Munn, J. Mol. Electronics **2**, 101 (1986).
5. G.G. Roberts, Advan. Phys. **34**, 475 (1985).
6. G. Decher, B. Tieke, C. Bosshard and P. Günter, conference abstract.
7. R.W. Munn, Mol. Phys. **64**, 1 (1988).
8. M.R. Philpott, J. Chem. Phys. **58**, 588 (1973).
9. R.W. Munn, S.E. Mothersdale and M.M. Shabat, in *Organic Materials for Nonlinear Optics II*, ed. R.A. Hann and D. Bloor, RSC Special Publication No. 91 (Royal Society of Chemistry, Cambridge, 1991), p.34.
10. F.W. de Wette and G.E. Schacher, Phys. Rev. **137**, A78 (1965).
11. P.G. Cummins, D.A. Dunmur, R.W. Munn and R.J. Newham, Acta Cryst. A32, 847 (1976).

Organic Materials for Nonlinear Optics III, in press

CALCULATIONS OF NLO RESPONSE IN LANGMUIR-BLODGETT FILMS

R.W. Munn and M.M. Shabat*

Department of Chemistry and Centre for Electronic Materials, UMIST, Manchester M60 1QD, U. K.
*(*Present address: Physics Department, Islamic University of Gaza, P. O. Box 108, Gaza, Gaza Strip, via Israel)*

1 INTRODUCTION

Organic materials are attractive for nonlinear optics because they offer the possibility of tailoring the molecules to modify their properties. However, this implies but also that one understands how the desired material properties arise from the molecular properties. The basic understanding is well established: the material response is given by the molecular response transformed from molecular to material axes, modified by local-field factors that relate the polarizing field in the material to the macroscopic electric field at the relevant frequencies.[1] Often the local-field factors are approximated by the Lorentz local-field factor using the mean refractive index, in the spirit of the oriented-gas model.[2] In crystals, this approximation is known to be reasonable for compact molecules but not for elongated ones,[3] and hence care needs to be taken in interpreting and predicting NLO response of ordered materials composed of markedly anisotropic molecules.

These reservations clearly apply to Langmuir-Blodgett films, formed from amphiphilic molecules with a hydrophilic "head" and a long hydrophobic "tail". The effect of the elongated structure on the local field is not obvious, particularly if the molecular axis is tilted away from the normal to the film, as often seems to occur.[4] Previous algebraic results show how a planewise approach can be used to calculate the linear and nonlinear optical response of layered materials such as LB films.[5] Here we report numerical calculations for simplified model LB films in order to explore how the response varies with molecular tilt and lattice distortion. This work forms part of a coordinated programme to design, prepare and characterize LB films with high NLO activity.[6]

2 MODEL STRUCTURE

The model is composed of molecules treated as a string of identical "beads" to represent their size, shape and orientation. The parent structure has the molecules in each layer of the film packed in a regular triangular array with their long axes perpendicular to the layer. Centring alternate layers so that molecules lie over the triangle formed by molecules in the preceding layer produces a hexagonal

structure. A plan view of the structure is shown in Figure 1.

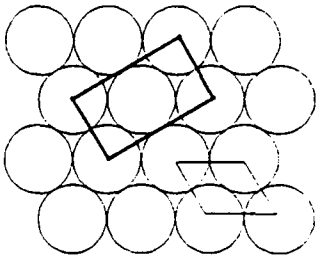

Figure 1. Plan view of layer showing bases of the hexagonal (light) and monoclinic (bold) cells.

Apart from the conventional hexagonal unit cell, the structure can also be described by the centred monoclinic cell indicated. Its short edge length is the nearest-neighbour (NN) distance D, and its long edge length is the next-nearest-neighbour (NNN) distance $\sqrt{3}D$, where D is the diameter of a "bead". When molecules tilt, it is necessary to specify not only the tilt but also the plane of tilt. It appears that NNN tilt prevails, and the monoclinic cell is then preferable. There are also indications from atomic-force microscopy that some LB films have a distorted hexagonal structure,[7] which is conveniently modelled by changing the axial ratio of the monoclinic cell. For multilayers, it is necessary to specify the relationship between tilts in successive layers, which may be the same or alternating, as shown in Figure 2.

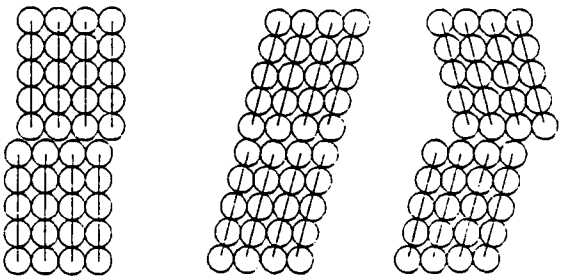

Figure 2. Elevation of structures showing successive layers without tilt, with the same tilt, and with alternating tilt.

3 METHOD

Interactions between molecules are expressed in terms of planewise dipole sums giving the field at a molecule in one layer due to dipoles on the molecules in that or another layer. These sums have been calculated using standard expressions.[8,9] They are calculated separately between all pairs of "beads" and then averaged to give molecular sums $T_{\alpha\beta}(g)$, where α and β are cartesian components and g is the number of layer spacings between the origin molecule and the layer of dipoles. Hence $g = 0$ denotes interactions within a layer, $g = 1$ interactions between adjacent layers, and so on. The sums are scaled by a factor $v/4\pi$, where v is the molecular volume, to give dimensionless quantities.

As reported below, interactions for $g \geq 1$ are very small, so that it suffices to consider only the sum T(0) and the corresponding planewise Lorentz-factor tensor $\mathsf{L} = \mathsf{T}(0) + \boldsymbol{nn}$, where $\boldsymbol{n}$ is the normal to the layers. The local polarizing electric field $\boldsymbol{F}$ is related to the macroscopic field $\boldsymbol{E}$ by

$$\boldsymbol{F} = (\mathsf{1} - \mathsf{L}\cdot\mathsf{a})^{-1}\cdot\boldsymbol{E} = \mathsf{d}\cdot\boldsymbol{E}, \tag{1}$$

where $\mathsf{a} = \alpha/\epsilon_0 v$ is a dimensionless reduced polarizability and d is the local-field tensor. The relative permittivity is

$$\epsilon = \mathsf{1} + \mathsf{a}\cdot\mathsf{d} = \mathsf{1} + \chi^{(1)} \tag{2}$$

where $\chi^{(1)}$ is the linear susceptibility, and in direction e the refractive index n_e is given by $1/n_e^2 = e\cdot\epsilon^{-1}\cdot e$.

The quadratic susceptibility is[5,10]

$$\chi^{(2)} = \mathsf{d}^{\mathsf{T}}\cdot\mathsf{b}:\mathsf{dd}, \tag{3}$$

where the superscript T denotes the transpose and $\mathsf{b} = \beta/\epsilon_0 v$ is a reduced molecular first hyperpolarizability. The cubic susceptibility comprises a *direct* term $\chi^{(3d)}$ and a *cascading* term $\chi^{(3c)}$:[5]

$$\chi^{(3)} = \mathsf{d}^{\mathsf{T}}\cdot\mathsf{c}:\mathsf{ddd} + 2\mathsf{d}^{\mathsf{T}}\cdot\mathsf{b}:\mathsf{dd}\cdot\mathsf{d}\cdot\mathsf{L}\cdot\mathsf{b}:\mathsf{dd} \equiv \chi^{(3d)} + \chi^{(3c)}, \tag{4}$$

where $\mathsf{c} = \gamma/\epsilon_0 v$ is a reduced molecular second hyperpolarizability.

The molecular response is treated in a simplified way designed to make changes of film structure the dominant influence on film response. In molecular axes $X\ Y\ Z$, the polarizability is taken as $(\alpha, \alpha, s\alpha)$, with $\alpha/\epsilon_0 v$ fixed as 0.2. The first hyperpolarizability is taken to have nonzero components β_{ZAB} diagonal in AB, with components $(\beta, \beta, -s\beta)$ diagonal in AB and $\beta/\epsilon_0 v$ fixed as 3.8 pm V^{-1}. The second hyperpolarizability is taken to have only the component $\gamma_{zzzz} = s\gamma$ nonzero, with $\gamma/\epsilon_0 v$ fixed as 200 (pm V^{-1})^2. These choices are guided by published calculations of molecular response.

4 RESULTS

Planewise dipole tensor sum components for $g = 0$ and 1 as a function of tilt are given in Table 1 for $s = 5$ relative to $x\ y\ z$ cartesian axes, where z is normal to the layers and xz is the plane of tilt. For $g = 1$, the values are at most 1% of the corresponding components for $g = 0$, and hence terms for $g \geq 1$ can be neglected. For $g = 0$ at zero tilt, the values give a diagonal Lorentz-factor tensor close to (0.5, 0.5, 0), the depolarization factor expected for a needle-shaped Lorentz cavity, consistent with the elongated molecular shape. Tilt affects L_{yy} little, but brings L_{xx} and L_{zz} close. Very similar results are obtained for

Table 1. Planewise sum components $T_{\alpha\beta}(g)$ for various tilts θ.

θ	$\alpha\beta$			
	xx	xz	yy	zz
$g = 0$				
0°	0.491	0	0.491	-0.982
20°	0.440	0.093	0.467	-0.907
40°	0.281	0.148	0.420	-0.701
$g = 1$				
0°	-0.0016	0	-0.0016	0.0031
20°	-0.0010	-0.0023	-0.0007	-0.0002
40°	0.0016	0.0011	0.0043	-0.0059

values of s up to 10, and so future results all refer to $s = 5$. The effect of distortion was explored by expanding one edge of the monoclinic cell base and contracting the other in the same proportion. Distortions up to 10% produced linear variations in the planewise sum components of similar proportions.

The local field component d_{yy} depends on tilt only through L_{yy} and so varies little, from 1.109 at zero tilt to 1.092 at 40° tilt. In the x and z directions, tilt affects the Lorentz-factor tensor and polarizability components in opposite senses, so there is also no great change. The local field component d_{xx} increases from 1.109 at zero tilt to 1.118 at 20° but then decreases to 1.100 at 40°, while d_{zz} increases from 1.018 at zero tilt to 1.064 at 20° and 1.166 at 40°. Off-diagonal components are always less than 0.05.

The refractive index n_y varies little with tilt because the polarizability along y does not change. The variation of the other refractive indices largely reflects that of the polarizability: n_x increases from 1.105 at zero tilt to 1.217 at 40°, and n_z decreases from 1.421 to 1.285. The principal directions in the xz plane remain within 1° of the molecular axes. Distortion of the lattice as described earlier has little effect on the refractive indices: 10% distortion at zero tilt changes n_x by +0.0009, n_y by -0.0007, and n_z by -0.0018.

Quadratic susceptibility components as a function of tilt are given in Table 2. The assumed form of β ensures Kleinman symmetry. The effects of tilt are marked, and monotonic except for χ_{xxx} where β_{xxx} changes sign as θ increases.

The direct parts of the cubic susceptibility components are given in Table 3. Tilt decreases the $zzzz$ component and increases the others in magnitude. Cascading parts are also given in Table 3 with β treated as having only an axial

Table 2. Quadratic susceptibility components $\chi_{\alpha\beta\gamma}$/pm V^{-1} for various tilts θ.

θ	$\alpha\beta\gamma$					
	xxx	*xxz*	*xyy*	*xzz*	*zyy*	*zzz*
0°	0	4.9	0	0	4.9	-20.9
20°	-3.8	0.2	-1.8	10.7	4.8	-18.5
40°	0.3	-8.8	-3.2	13.5	4.2	-8.3

component, like γ. These parts reinforce the direct ones, except for χ_{zzzz} where they tend to offset the decreases with tilt, and are typically a quarter of the magnitude at 20° tilt and over half at 40°. Including all components of β complicates the pattern by introducing numerous additional components, the largest being χ_{yyyy} which reaches 5700 (pm V^{-1})^2 at 40° tilt, and modifying others, notably χ_{zzzz} which reaches 11 900 (pm V^{-1})^2.

Table 3. Cubic susceptibility components $\chi_{\alpha\beta\gamma\delta}$/(pm V^{-1})^2 for various tilts θ.

θ	$\alpha\beta\gamma\delta$				
	xxxx	*xxxz*	*xxzz*	*xzzz*	*zzzz*
Direct contribution					
0°	0	0	0	0	10800
20°	200	-600	1500	-3900	10500
40°	2100	-2800	3600	-4800	6300
Cascading contribution					
0°	0	0	0	0	200
20°	100	-200	400	-1100	2900
40°	1300	-1700	2300	-3000	4000

5 DISCUSSION

The numerical values used in the present work are arbitrary but plausible. Hence a number of the qualitative results should be fairly widely applicable.

For elongated molecules, dipolar interactions between different layers are essentially negligible, even for a tilt as large as 40°. This greatly simplifies the dielectric theory. The local fields are surprisingly little affected by tilt, so that the linear susceptibility and refractive indices are determined largely by the

relevant components of the effective polarizability. Birefringence measurements could thus provide reliable information on tilt, but probably not on lattice distortion.

The nonlinear susceptibilities can be fairly readily interpreted in terms of the effect of tilt on the molecular polarizability referred to the film x y z axis system. The lower symmetry of the tilted structures produces a much more complex set of components and correspondingly requires a more complicated interpretation of measurements, especially since components induced by tilt can be comparable with those for zero tilt. In the cubic susceptibility, the cascading terms can be as large as the direct terms, so that a simple interpretation based solely on the second hyperpolarizability may be misleading.

Future work is required on more realistic molecular structures in which the response is not assumed to be uniformly distributed but is concentrated in the NLO chromophore.

ACKNOWLEDGEMENTS

This work was supported by DARPA contract no. DAJA 45-89-C-0036. Calculations on distorted structures were performed by S.J. Collins and J.C. Boxall.

REFERENCES

1. J.A. Armstrong, N. Bloembergen, J. Ducuing and P.S. Pershan, Phys. Rev., 1961, **127**, 1918.
2. J. Badan, R. Hierle, A. Périgaud and J. Zyss, in *Nonlinear Optical Properties of Organic and Polymeric Materials*, ed. D.J. Williams, ACS Symposium Series **233** (American Chemical Society, Washington, 1983), p. 81.
3. J.H. Meyling, P.J. Bounds and R.W. Munn, *Chem. Phys. Letters*, 1977, **51**, 234.
4. M.C. Petty, in *Langmuir Blodgett Films*, ed. G.G. Roberts (Plenum, New York, 1990), p. 133.
5. R.W. Munn, S.E. Mothersdale and M.M. Shabat, in *Organic Materials for Nonlinear Optics II*, eds R.A. Hann and D. Bloor, RSC Special Publication No. **91** (Royal Society of Chemistry, Cambridge, 1991), p. 34.
6. M. Bishop, J.H.R. Clarke, L.E. Davis, T.A. King, F.R. Mayers, A. Mohebati, R.W. Munn, M.M. Shabat, D. West and J.O. Williams. *Thin Solid Films*, 1992, **210/211**, 185.
7. L. Bourdieu, P. Silberzan and D. Chatenay, *Phys. Rev. Lett.*, 1991, **67**, 2029.
8. F.W. de Wette and G.E. Schacher, *Phys. Rev.*, 1965, **137**, A78.
9. M.R. Philpott, *J. Chem. Phys.*, 1973, **58**, 588.
10. R.W. Munn and M.M. Shabat, in *Molecular Electronics - Science and Technology II*, ed. A. Aviram (American Institute of Physics, in press).